

Robust \mathcal{H}_∞ control and worst-case search in constrained parametric space

Ervan Kassarian¹, Francesco Sanfedino², Daniel Alazard², Andrea Marrazza¹

Abstract

Standard $\mathcal{H}_\infty/\mathcal{H}_2$ robust control and analysis tools operate on uncertain parameters assumed to vary independently within prescribed bounds. This paper extends their capabilities in the presence of constraints coupling these parameters and restricting the parametric space. Focusing on the worst-case search, we demonstrate – based on the theory of upper- C^1 functions – the validity of using standard, readily available smooth optimization algorithms to address this nonsmooth constrained optimization problem. Accordingly, we propose to explore the parametric space with either Monte-Carlo sampling or particle swarm optimization, and to subsequently perform local exploitation with Sequential Quadratic Programming to compute Karush-Kuhn-Tucker points. This worst-case search then enables robust controller synthesis: as in the state-of-art algorithm for standard robust control, identified worst-case configurations are iteratively added to an active set on which a non-smooth multi-models optimization of the controller is performed. The methodology is illustrated on a satellite benchmark with flexible appendages, of order 50 with 43 uncertain parameters. We show that the proposed method largely outperforms Monte-Carlo sampling alone, is able to reliably detect even rare worst-case configurations in minutes on a standard laptop, and that the robust controller optimization converges with less than 10 active configurations. Even in the unconstrained case, the proposed framework complements traditional methods, as it scales to plants with many parameters and states and explores the entire parametric space, albeit without formal guarantees of global optimality.

I. INTRODUCTION

The standard robust structured \mathcal{H}_∞ control problem [1] is formulated as the min-max optimization problem:

$$\underset{K \in \mathcal{K}}{\text{minimize}} \quad \max_{\delta \in \mathcal{D}} \|T_{zw}(s, K, \delta)\|_\infty \quad (1)$$

where $T_{zw}(s, K, \delta)$ is a transfer function between input w and output z , K is the controller to be optimized, \mathcal{K} is the set of controllers of the chosen structure, and δ is the vector of k uncertain parameters in a parametric space \mathcal{D} . A multi-objective formulation can also be stated as follows:

$$\begin{aligned} &\underset{K \in \mathcal{K}}{\text{minimize}} \quad \max_{\delta \in \mathcal{D}} \|T_{z_1 w_1}(s, K, \delta)\| \\ &\text{subject to} \quad \max_{\delta \in \mathcal{D}} \|T_{z_i w_i}(s, K, \delta)\| \leq 1, \quad 2 \leq i \leq n \end{aligned} \quad (2)$$

where $\|\cdot\|$ may refer to the \mathcal{H}_2 or \mathcal{H}_∞ system norm. The channel $w_1 \rightarrow z_1$ corresponds to a "soft" requirement to be minimized, while the other channels $w_i \rightarrow z_i$ ($i > 1$) are "hard" requirements, that must be inferior to 1 (once normalized) but not necessarily minimized.

In this paper, we mainly focus on the inner maximization problems, namely search for worst-case performance:

$$\max_{\delta \in \mathcal{D}} \|T_{zw}(s, K, \delta)\| \quad (3)$$

and worst-case stability – stability is implicitly required to ensure finite norms – treated as in [2]:

$$\max_{\delta \in \mathcal{D}} \alpha(A(K, \delta)) \quad (4)$$

where $A(K, \delta)$ is the matrix A of the state-space representation of the closed-loop system, and $\alpha(\cdot)$ denotes the spectral abscissa:

$$\alpha(M) := \max\{\text{Re}(\lambda) : \lambda \text{ is an eigenvalue of } M\}.$$

Classically in the literature, \mathcal{D} is the hypercube $[-1, 1]^k$ after normalization of the uncertain parameters, and $T_{zw}(s, K, \delta)$ is modeled under the Linear Fractional Representation (LFR). In this case, MATLAB's function SYSTUNE, relying on the non-smooth optimization of [2], [3], is now widely used in academia and industry to solve problems (1) and (2). More specifically, in [2], problems (3) and (4) are solved with local non-smooth optimization. Indeed, the computation of Clarke subdifferentials [4] of the spectral abscissa and of the \mathcal{H}_∞ norm [5] enables a bundle method to quickly find worst-case configurations with regard to stability and performance. The control problem (1) is then tackled by combining this worst-case search with the non-smooth controller optimization of [3]. This approach relies on the construction of an inner approximation $\mathcal{D}_a \subset \mathcal{D}$ composed of so-called active configurations. At each iteration, the controller is tuned so as to be robust to all current active configurations. Then, a worst-case search is performed; if the worst-case configuration does not satisfy the control requirements, it is added to \mathcal{D}_a and the algorithm goes back to controller tuning; otherwise, the algorithm can terminate.

¹DYCSYT, 10 Avenue Marc Péglerin, 31400 Toulouse, France.

²Fédération ENAC ISAE-SUPAERO ONERA, Université de Toulouse, 10 Avenue Marc Péglerin, Toulouse, 31400, France

It is shown that this approach is both more reliable and more efficient than gridding the parametric space, which quickly becomes intractable when the number of parameters increases. In practice, the optimization generally finishes with a small number of active configurations. As this approach relies on local searches, robustness is generally thoroughly verified a posteriori. μ -analysis [6] was developed for this purpose, generally based on branch-and-bound algorithms [7]. It provides guaranteed deterministic lower and upper bounds of the global optimum; a probabilistic variant also exists [8], [9]. Monte-Carlo sampling can also guarantee a probability of robustness within predefined thresholds of accuracy and confidence [10]. Another common industrial practice is to grid the parametric space with a limited number of samples, typically 100 to 1000 combinations of the parameters bounds. But this approach will miss any worst case occurring between grid points and, unlike Monte-Carlo, does not provide any statistical guarantee.

This paper addresses the case where nonlinear constraints, noted $c_i(\delta) \leq 0$ and possibly including equality constraints, restrict the hypercube:

$$\mathcal{D} = \{\delta \in [-1, 1]^k \text{ s.t. } c_i(\delta) \leq 0, 1 \leq i \leq n\} \quad (5)$$

Our focus is twofold. Firstly, we seek computationally efficient techniques that can be integrated into robust control design, alternating between multi-models controller synthesis and worst-case search as in [2], to solve the standard problem (1) and its multi-objectives formulation (2) in reasonable time. Secondly, we aim to assess their reliability in consistently detecting global worst-case configurations as a validation tool.

The robust control and analysis approaches discussed above do not address the constrained case, at least not in their current implementations. Nevertheless, quantifying robustness can still be approached with Monte-Carlo sampling; samples that do not satisfy the nonlinear constraint are simply discarded. Evaluating the stability or the norm of a linear system at a given parametric configuration is relatively fast, and easily parallelizable; moreover, the number of evaluations required to provide the desired levels of probability and confidence is independent from the number of parameters [10]. However, finding a worst case, e.g. to address problems (3) or (4), may require numerous function evaluations and lead to a significant computation time, especially in critical systems for which even rare worst cases must be avoided. This is particularly an issue when the robustness analysis iterates with controller design to perform robust tuning.

In this paper, we demonstrate new properties of the class of upper- C^1 functions [11], and in particular the convergence of Sequential Quadratic Programming (SQP) [12], a standard constrained optimization algorithm, when applied to such functions even though they are not smooth. We deduce that SQP can be applied to the nonsmooth problem (3), and to (4) under an additional assumption. Then, relying on built-in MATLAB functions, we propose to explore the parametric space with either Particle Swarm Optimization (PSO) [13], tackling the nonlinear constraint through a penalty approach [14], or Monte-Carlo sampling (if stochastic guarantees are sought), and subsequently refine the search with SQP to find Karush-Kuhn-Tucker points of the optimization problem. Then, following the approach of [2], this worst-case search method is then combined with multi-models controller optimization [3] to perform robust control. To the best of our knowledge, this is the first robust \mathcal{H}_∞ control approach that tackles nonlinear constraints on the uncertain parameters.

We emphasize that the proposed techniques, although studied here in the context of the constrained space (5), may also prove valuable in the unconstrained case. Indeed, μ -analysis remains difficult to apply to industrial systems with many uncertain parameters – as illustrated in the recent references [15], [16], [17], [18] where systems with 16 to 20 parameters required sensitivity-based model reduction to make the problem tractable, at the expense of model fidelity. In particular, [19] shows that such μ -analysis can even lead to an overly optimistic worst-case prediction after model reduction. This occurs because the formal robustness guarantees apply only to the reduced model and do not extend to the original system, thus limiting the practical value of sensitivity-based μ -analysis. By contrast, the proposed approach scales well to plants with many states and parameters, and thus can be applied to the full system. Furthermore, the non-smooth optimization of [2], implemented in SYSTUNE, is local and sometimes misses worst-case configurations, whereas the proposed approach performs a global exploration of the parametric space, albeit without formal guarantees of global optimality.

We illustrate the proposed approach on the robust control of a spacecraft with flexible appendage. In such systems, uncertainties associated with the mechanical properties of flexible appendages must satisfy a condition of the form (5) or otherwise be excluded from robustness analysis (specifically, the residual mass matrix must remain positive definite). While structured \mathcal{H}_∞ control has become industrial standard practice among satellite integrators for missions with demanding control requirements [17], [20], [21], [22], this constraint, and more generally the robustness analysis, is generally handled using Monte-Carlo or gridding approaches, which suffer from the aforementioned drawbacks. The proposed methodology offers a practical and scalable alternative that can significantly reduce engineering effort and computational cost.

II. CONSTRAINED OPTIMIZATION OF UPPER- C^1 FUNCTIONS

A. Properties of upper- C^1 functions

In this section, we introduce the class of upper- C^1 functions and demonstrate favorable properties for their minimization. This will be relevant for the robust control problem, which, as we shall see, involves such functions. For readability and

since our primary focus is on robust control, proofs that result from adapting existing arguments from the differentiable to the upper- C^1 functions are only provided in Appendix.

Definition 1 (Lower- and upper- C^1 functions [11])

A locally Lipschitz function $f : \mathbb{R}^n \rightarrow \mathbb{R}$ is upper- C^1 at $x \in \mathbb{R}^n$ if there exists a compact set S , a neighborhood U of x , and a function $F : U \times S \rightarrow \mathbb{R}$ such that F and $\nabla_x F$ are jointly continuous in x and s , and such that

$$f(x) = \min_{s \in S} F(x', s) \quad \text{for all } x' \in U.$$

We note $I(x)$ the subset of S that defines the active functions $F(\cdot, s)$ at x , i.e.:

$$I(x) = \arg \min_{s \in S} F(x, s) = \{s \in S, f(x) = F(x, s)\}.$$

f is lower- C^1 if $-f$ is upper- C^1 , i.e. f can be written as a maximum, similarly to the expression above.

[2, Sections III.A., II.B., V.A.] shows that minimization of such upper- C^1 functions, even when not differentiable everywhere, exhibits similar behavior to smooth functions. In particular, the authors show the convergence of their bundle method, in the search of the worst-case \mathcal{H}_∞ norm, even when the cutting plane step is reduced to a standard linesearch (as in smooth optimization). This work follows [23] that treats of the optimization of lower- and upper- C^1 functions. Similar considerations are also thoroughly discussed by the same authors in [24]. Similarly, in [25], the Frank-Wolfe algorithm, originally designed for smooth functions, is also proven to converge to Clarke-stationary points when applied to upper- C^1 functions. In the same spirit, we now show that the upper- C^1 functions, although not differentiable everywhere, maintain some favorable properties for their minimization. Then, we will demonstrate the convergence of one particular smooth optimization algorithm when applied to upper- C^1 functions.

In this whole Section, we consider $f : \mathbb{R}^k \rightarrow \mathbb{R}$ an upper- C^1 function. Let us first consider the unconstrained problem:

$$\underset{x \in \mathbb{R}^k}{\text{minimize}} \quad f(x) \tag{6}$$

Proposition 1 (Descent directions and optimality of upper- C^1 functions – Unconstrained case)

Let a locally Lipschitz function f be upper- C^1 at x , and $g_x \in \partial f(x)$ any subgradient of f at x . We consider Problem (6).

- a) Descent direction. Any direction $-g_x$, with $g_x \in \partial f(x)$ such that $\|g_x\| \neq 0$, is a descent direction for $f(x)$, and in particular it verifies $f'(x, -g_x) \leq -\|g_x\|^2 < 0$ where $f'(x, d)$ denotes the directional derivative at x in direction d .
- b) Optimality. If x (locally) minimizes $f(x)$, then $\|g_x\| = 0$ for any $g_x \in \partial f(x)$.

Proof. a) [25, Proposition 2 and equation (6)] shows that the directional derivative of an upper- C^1 function f is:

$$f'(x, d) = \min_{g \in \partial f(x)} \langle g, d \rangle = \min_{u \in I(x)} \langle \nabla_x F(x, u), d \rangle \tag{7}$$

where $\langle \cdot, \cdot \rangle$ denotes the scalar product. From equation (7), $f'(x, -g_x) = \min_{g \in \partial f(x)} (-g^T g_x) \leq -g_x^T g_x = -\|g_x\|^2 \leq 0$ and the last inequality is strict when $\|g_x\| \neq 0$.

- b) If x minimizes f , then $f'(x, -g_x) \geq 0$. But, by a), $f'(x, -g_x) \leq -\|g_x\|^2$. Thus, $\|g_x\| = 0$. \square

Proposition 1.a) shows that when a smooth optimization algorithm is provided with any subgradient as if it were the gradient of a smooth function, progress can still be achieved at points of nonsmoothness, owing to the regularity property of upper- C^1 functions. Naturally, the selected direction is not necessarily the steepest descent. Proposition 1.b) ensures that an optimization algorithm can rely on the same optimality conditions as in the smooth case when picking any subgradient (we recall that, for the general case of nonsmooth functions, the optimality condition is $0 \in \partial f(x)$, which is a weaker condition).

We shall now demonstrate similar results for the constrained problem:

$$\begin{aligned} &\underset{x \in \mathbb{R}^k}{\text{minimize}} && f(x) \\ &\text{subject to} && c_i(x) \leq 0, \quad 1 \leq i \leq n \end{aligned} \tag{8}$$

where the c_i are differentiable, and f is upper- C^1 . We do not consider equality constraints, as they can be written equivalently as two inequality constraints. The Karush-Kuhn-Tucker (KKT) conditions of Problem (8) read: there exists $g_x \in \partial f(x)$ and $(u_i)_{1 \leq i \leq n}$ such that:

$$\begin{aligned} g_x + \sum_{i=1}^n u_i \nabla c_i(x) &= 0 \\ \forall i, u_i &\geq 0, u_i c_i(x) = 0, c_i(x) \leq 0 \end{aligned} \tag{9}$$

We also consider the quadratic problem:

$$Q(x, H, g_x) : \begin{array}{ll} \underset{p \in \mathbb{R}^k}{\text{minimize}} & g_x^T p + \frac{1}{2} p^T H p \\ \text{subject to} & c_i(x) + \nabla c_i(x)^T p \leq 0, \quad 1 \leq i \leq n \end{array} \quad (10)$$

where H is a symmetric definite positive matrix and $g_x \in \partial f(x)$. The quadratic problem $Q(x, H, g_x)$ can be seen as a local approximation of the Problem (8) where the matrix H may contain information about the curvature of both objective and constraint functions, usually serving as an approximation of the Lagrangian. $Q(x, H, g_x)$ is originally introduced in methods such as [26] where f is differentiable and $\nabla f(x)$ replaces g_x .

Finally, for $r \geq 0$, we introduce the *merit function* θ_r as in [26]:

$$\theta_r(x) = f(x) + r \sum_{i=1}^n c_i(x)_+ \quad (11)$$

where $c_i(x)_+ = \max(0, c_i(x))$.

Proposition 2 (Descent directions and optimality of upper- C^1 functions – Constrained case)

Let a locally Lipschitz function f be upper- C^1 at x , and $g_x \in \partial f(x)$ any subgradient of f at x . Let the c_i be continuously differentiable. We consider Problem (8).

a) Descent direction. Let (p, u) be a KKT pair of $Q(x, H, g_x)$. If $\|p\| \neq 0$ and $\|u\|_\infty \leq r$, then p is a descent direction for $\theta_r(x)$, i.e. $\theta'_r(x, p) < 0$ where $\theta'_r(x, d)$ denotes the directional derivative at x in direction d .

b) Optimality. If x (locally) minimizes $f(x)$ subject to n constraints $c_i(x) \leq 0$ (Problem (8)), then any $g_x \in \partial f(x)$ verifies the following KKT conditions: there exists $(\mu_i)_{1 \leq i \leq n}$ such that:

$$\begin{aligned} g_x + \sum_{i=1}^n \mu_i \nabla c_i(x) &= 0 \\ \forall i, \mu_i &\geq 0, \mu_i c_i(x) = 0, c_i(x) \leq 0 \end{aligned}$$

Proof. a) Cf. Appendix. The proof is a mere adaptation of [26, Theorem 3.1] to the upper- C^1 case.

b) Let us note $\mathcal{C} = \{x, c_i(x) \leq 0 \forall i\}$. Since x is a local minimizer of $f(x)$ in \mathcal{C} , there exists a ball $B(x, r_1)$ of radius $r_1 > 0$ and of center x such that $f(x') \geq f(x)$ for all $x' \in B(x, r_1) \cap \mathcal{C}$. Recall that U is the neighborhood of x of Definition 1; as $B(x, r_1)$ and U are both non-empty neighborhoods of x , we can define $r_2 > 0$ such that $B(x, r_2) \subset B(x, r_1) \cap U$. Let us consider any of the functions $F(\cdot, s)$. For all $x' \in B(x, r_2) \cap \mathcal{C}$, we have $F(x', s) \geq f(x') \geq f(x)$, where the first inequality follows from $x' \in U$, and the second from $x' \in B(x, r_1) \cap \mathcal{C}$. Assuming additionally that $F(\cdot, s)$ is active, i.e. $s \in I(x)$, then $F(x, s) = f(x)$ and we conclude that $F(x', s) \geq F(x, s)$ for all $x' \in B(x, r_2) \cap \mathcal{C}$.

This shows that x locally minimizes all active functions $F(\cdot, s)$ under the constraints $c_i(x) \leq 0$. Therefore, these functions verify the following KKT conditions: for all $s \in I(x)$, there exists $(\lambda_i(s))_{1 \leq i \leq n}$ such that:

$$\begin{aligned} \nabla_x F(x, s) + \sum_{i=1}^n \lambda_i(s) \nabla c_i(x) &= 0 \\ \forall i, \lambda_i(s) &\geq 0, \lambda_i(s) c_i(x) = 0, c_i(x) \leq 0 \end{aligned}$$

As shown in [4], [25], the subdifferential of an upper- C^1 function f at x is the convex hull formed by the gradients of the active functions $F(\cdot, s)$:

$$\partial f(x) = \text{co} \{ \nabla_x F(x, s) : s \in I(x) \}$$

Thus, $g_x \in \partial f(x)$ can be written as:

$$g_x = \sum_{j=1}^p a_{s_j} \nabla_x F(x, s_j), \quad s_j \in I(x) \quad \forall j$$

where the $a_{s_j} \geq 0$ are such that $\sum_{j=1}^p a_{s_j} = 1$ (and p is at most the number of parameters plus one). Then, we have:

$$g_x = - \sum_{j=1}^p a_{s_j} \sum_{i=1}^n \lambda_i(s_j) \nabla c_i(x) = - \sum_{i=1}^n \left(\sum_{j=1}^p a_{s_j} \lambda_i(s_j) \right) \nabla c_i(x) = - \sum_{i=1}^n \mu_i \nabla c_i(x)$$

where $\mu_i := \sum_{j=1}^p a_{s_j} \lambda_i(s_j)$. For all i : $\mu_i \geq 0$ (because all a_{s_j} and $\lambda_i(s_j)$ are ≥ 0), and $\mu_i c_i(x) = 0$ (because if $c_i(x) \neq 0$, then all $\lambda_i(s_j)$ are 0). This proves Proposition 2.b). \square

Remark 1. Proposition 1.b) is similar to [25, Proposition 4], where it is shown that "directional-stationarity", i.e. the assumption that $f'(x, d) \geq 0$ for any $d \in \mathbb{R}^k$, implies that all subgradients are 0. Note that directional stationarity does not imply that x minimizes $f(x)$; for this, more assumptions would be required, e.g. convexity of the $F(\cdot, s)$ [25, Theorem 10]. Proposition 2.a) is a generalization of [26, Theorem 3.1], originally for differentiable functions, to upper- C^1 functions. To

the best of our knowledge, Proposition 2.b) is novel, and can also be seen as a specific case of the usual KKT conditions for upper- C^1 functions. It allows optimality to be checked with any subgradient, in contrast to the general nonsmooth case, where only the existence of one subgradient satisfying KKT conditions is required.

B. Convergence of sequential quadratic programming (SQP) for upper- C^1 functions

We now introduce the Sequential Quadratic Programming (SQP) algorithm to solve Problem (8). It is described in Algorithm 1, as in [26] except that we replaced the gradient $\nabla f(x)$ by any subgradient $g_x \in \partial f(x)$ in the quadratic problem $Q(x, H, g_x)$ (equation (10)). See also [27] for a discussion when the penalty parameter r is variable. We do not detail how the quadratic problem in Step 1 or the step size λ_k in Step 2 may be solved, or how H_k is updated in Step 3, as it does not affect the convergence proof (as long as the conditions described in Algorithm 1 are satisfied)

Algorithm 1 Sequential Quadratic Programming (SQP) algorithm [26] for upper- C^1 functions

Initialization: $x_0 \in \mathbb{R}^k$, $H_0 \in \mathbb{R}^{k \times k}$ positive definite, $r > 0$, $\lambda_{max} > 0$.

Step 1: Pick a $g_{x_k} \in \partial f(x_k)$. Find a KKT point p_k of the quadratic problem $Q(x_k, H_k, g_{x_k})$ defined in equation (10).

Step 2: Set $x_{k+1} = x_k + \lambda_k p_k$ for any $\lambda_k \in [0, \lambda_{max}]$ satisfying:

$$\theta_r(x_{k+1}) \leq \min_{0 \leq \lambda \leq \lambda_{max}} \theta_r(x_k + \lambda p_k) + \epsilon_k$$

where θ_r is defined in equation (11), and (ϵ_k) is a sequence of nonnegative numbers satisfying:

$$\sum_{i=0}^{\infty} \epsilon_i < \infty$$

Step 3: Update H_{k+1} by some scheme that keeps it definite positive.

Proposition 3 extends the convergence result of SQP established in [26, Theorem 3.2] for differentiable objective functions to the case of upper- C^1 objective functions. Besides the upper- C^1 condition of f , the same assumptions as in [26, Theorem 3.2] are considered.

Proposition 3 (Convergence of SQP for upper- C^1 functions)

Let f be upper- C^1 and the c_i be continuously differentiable. Assume that the following conditions are satisfied:

(i) there exists $\alpha, \beta > 0$ such that, for each k and for any $x \in \mathbb{R}^k$:

$$\alpha x^T x \leq x^T H_k x \leq \beta x^T x$$

(ii) For each k , there exists a KKT point of $Q(x_k, H_k, g_{x_k})$ (equation (10)) with a Lagrange multiplier vector u_k such that $\|u_k\|_{\infty} \leq r$ (vector ∞ -norm).

Then, any sequence (x_k) generated by Algorithm 1 either terminates at a KKT point of the constrained optimization problem (8), or any accumulation point \bar{x} with

$$S^0(\bar{x}) = \{p : c(\bar{x}) + \nabla c(\bar{x})^T p < 0\} \neq \emptyset$$

is a KKT point of Problem (8).

Proof. Cf. Appendix. The proof follows that of [26, Theorem 3.2] and adapts it to the case where f is not differentiable but only upper- C^1 . In particular, the upper semi-continuity of the Clarke subdifferential allows to maintain the argument linked to the continuity of the gradient in the original proof. The existence of an accumulation point of the solutions p_k of the quadratic problems $Q(x_k, H_k, g_{x_k})$ also follows from the submonotonicity of the subdifferential of lower- C^1 functions [11] (cf. Lemma 1 in Appendix). \square

Proposition 2.b) establishes that local minima are necessarily KKT points for any subgradient, and Proposition 3 proves the convergence to KKT points when using any subgradient. Consequently, the standard SQP algorithm can be applied to upper- C^1 functions, by providing any subgradient where the gradient is expected.

Remark 2. The purpose of our arguments for using smooth optimization is not to claim superiority over specialized nonsmooth optimization methods. Instead, we emphasize that readily available algorithms (e.g., in MATLAB or Python toolboxes) can be applied successfully and produce satisfactory results.

III. WORST CASE SEARCH IN CONSTRAINED PARAMETRIC SPACE

A. Problem formulation

In this section, the controller K is fixed and, thus, voluntarily omitted in the notations.

As in [2], worst-case stability is studied by maximizing the spectral abscissa of the closed-loop matrix $A(\delta)$. The problem (4) can also be written as the following constrained optimization problem:

$$\begin{aligned} & \underset{\delta \in \mathbb{R}^k}{\text{minimize}} && a(\delta) := -\alpha(A(\delta)) \\ & \text{subject to} && -1 \leq \delta_i \leq 1 \\ & && c_i(\delta) \leq 0 \end{aligned} \quad (12)$$

Similarly for the performance problem (3), we define for the \mathcal{H}_∞ norm of a generic transfer function $T_{zw}(s, \delta)$:

$$\begin{aligned} & \underset{\delta \in \mathbb{R}^k}{\text{minimize}} && h_\infty(\delta) := -\|T_{zw}(s, \delta)\|_\infty \\ & \text{subject to} && -1 \leq \delta_i \leq 1 \\ & && c_i(\delta) \leq 0 \end{aligned} \quad (13)$$

and for the (squared) \mathcal{H}_2 norm:

$$\begin{aligned} & \underset{\delta \in \mathbb{R}^k}{\text{minimize}} && h_2(\delta) := -\|T_{zw}(s, \delta)\|_2^2 \\ & \text{subject to} && -1 \leq \delta_i \leq 1 \\ & && c_i(\delta) \leq 0 \end{aligned} \quad (14)$$

B. Properties of the objective functions

In this section, we consider a generic transfer function written as the Linear Fractional Transformation (LFT) [28, Chapter 10] $T_{zw}(s, \delta) = \mathcal{F}_u(M(s), \Delta)$, as depicted in Figure 1, where $\Delta = \text{diag}(\delta_i I_{n_i})$ (n_i is the number of repetitions of δ_i). This representation will be used to characterize either the internal stability, or the \mathcal{H}_∞ or \mathcal{H}_2 norm of the transfer from w to z ; practical problems e.g. (2) can also be addressed after an appropriate partitioning.

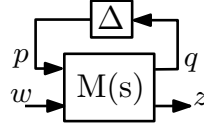


Fig. 1: LFT representation of T_{zw}

The state-space representation of $M(s)$ is written as:

$$\left\{ \begin{array}{l} \begin{bmatrix} \dot{x} \\ q \\ z \end{bmatrix} = \begin{bmatrix} A_1 & B_1 & B_2 \\ C_1 & D_{11} & D_{12} \\ C_2 & D_{21} & D_{22} \end{bmatrix} \begin{bmatrix} x \\ p \\ w \end{bmatrix} \\ p = \Delta q \end{array} \right\} \iff \left\{ \begin{array}{l} \begin{bmatrix} \dot{x} \\ \tilde{q} \\ z \end{bmatrix} = \begin{bmatrix} A_1 & B_1 & B_2 \\ \tilde{C}_1 & 0 & D_{12} \\ C_2 & D_{21} & D_{22} \end{bmatrix} \begin{bmatrix} x \\ \tilde{p} \\ w \end{bmatrix} \\ \tilde{p} = \tilde{\Delta} \tilde{q} \end{array} \right\}$$

where, in the right equation, the system was rewritten with the change of variable:

$$\tilde{\Delta} = (I - \Delta D_{11})^{-1} \Delta = \Delta (I - D_{11} \Delta)^{-1} \quad (15)$$

to have no direct transfer from \tilde{p} to \tilde{q} . This change of variable is the same as in [28, Section 12.3.4], with the uncertainty block instead of a feedback controller, and will be useful to study the \mathcal{H}_2 norm.

1) \mathcal{H}_2 norm (function h_2):

Proposition 4 (Differentiability of h_2)

Let us assume $D_{22} = 0$, and either $D_{12} = 0$ or $D_{21} = 0$. Then, h_2 is defined and differentiable in

$$\mathcal{D}_s = \{\delta \in \mathcal{D}, T_{zw}(s, \delta) \text{ is internally stable}\}$$

and its gradient is given in equation (18).

Proof. The assumption $D_{22} = 0$ is necessary to ensure finiteness of the \mathcal{H}_2 norm in the nominal case $\Delta = 0$. The assumption $D_{12} = 0$ or $D_{21} = 0$ is done for the same reason for $\Delta \neq 0$. The differentiability of h_2 in $\mathcal{D}_s = \{\delta \in \mathcal{D}, T_{zw}(s, \delta) \text{ is stable}\}$ was shown in [29, Section 3]; it was originally derived for a controller rather than an uncertainty block, but the validity

of the result extends straightforwardly to the latter. Let us write the state-space matrices of the transfer from w to z after closing the loop between p and q :

$$A(\delta) = A_1 + B_1 \tilde{\Delta} C_1, \quad B(\delta) = B_2 + B_1 \tilde{\Delta} D_{12}, \quad C(\delta) = C_2 + D_{21} \tilde{\Delta} C_1, \quad D(\delta) = D_{21} \tilde{\Delta} D_{12} = 0 \quad (16)$$

Then, the squared \mathcal{H}_2 norm is:

$$\|T_{zw}(s, \delta)\|_2^2 = \text{Tr} (B(\delta)^T X(\delta) B(\delta)) = \text{Tr} (C(\delta) Y(\delta) C(\delta)^T)$$

where $X(\delta)$ and $Y(\delta)$ are solutions of the Lyapunov equations:

$$\begin{aligned} A(\delta)^T X(\delta) + X(\delta) A(\delta) + C(\delta)^T C(\delta) &= 0 \\ A(\delta) Y(\delta) + Y(\delta) A(\delta)^T + B(\delta) B(\delta)^T &= 0. \end{aligned}$$

The derivative of h_2 at point δ for the variable $\tilde{\Delta}$, noted $h'_2(\tilde{\Delta})d\tilde{\Delta}$, is obtained from [30, Lemma 3.1] or equivalently [31, Section 2.1], also originally derived for a controller and adapted here for the uncertain block $\tilde{\Delta}$:

$$h'_2(\tilde{\Delta})d\tilde{\Delta} = \text{Tr} \left(\nabla_{\tilde{\Delta}} h_2(\delta)^T d\tilde{\Delta} \right)$$

where the gradient $\nabla_{\tilde{\Delta}} h_2(\delta)$ is given in the same references:

$$\nabla_{\tilde{\Delta}} h_2(\delta) = -2 (B_1^T X(\delta) + D_{21}^T C(\delta)) Y(\delta) C_1^T - 2 B_1^T X(\delta) B(\delta) D_{12}^T.$$

Finally, differentiating equation (15):

$$d\tilde{\Delta} = (I - \Delta D_{11})^{-1} d\Delta (I + D_{11}(I - \Delta D_{11})^{-1} \Delta)$$

and using the same notation as in [2]:

$$\Delta_i := \frac{\partial \Delta}{\partial \delta_i}, \quad (17)$$

the derivatives of h_2 read:

$$\frac{\partial h_2}{\partial \delta_i} = -2 \text{Tr} \left(\nabla_{\tilde{\Delta}} h_2(\delta)^T (I - \Delta D_{11})^{-1} \Delta_i (I + D_{11}(I - \Delta D_{11})^{-1} \Delta) \right). \quad (18)$$

□

2) \mathcal{H}_∞ norm (function h_∞):

Proposition 5 (Regularity of h_∞ [5], [3], [2])

a) h_∞ is locally Lipschitz and thus Clarke subdifferentiable (in the sense of [4]) everywhere in

$$\mathcal{D}_s = \{\delta \in \mathcal{D}, T_{zw}(s, \delta) \text{ is internally stable}\}.$$

b) h_∞ is upper- C^1 everywhere in \mathcal{D}_s .

c) h_∞ is differentiable in \mathcal{D}_s when only one frequency is active and of multiplicity one; in this case, its gradient is given in equation (19).

Proposition 5.a) is proved in [2, Proposition 1] and follows the work of [5] and [3]. The general subdifferential expression is provided in these references, but we will not use it in this paper. b) is proved in [2, Proposition 2]. c) immediately follows from a), and the expression is also provided in [2, Remark 5]: using the same notations, let us define T_{qw} and T_{zp} as:

$$\left[\begin{array}{c|c} * & T_{qw}(s, \delta) \\ \hline T_{zp}(s, \delta) & T_{zw}(s, \delta) \end{array} \right] = \left[\begin{array}{c|c} 0 & I \\ \hline I & \Delta \end{array} \right] \star M(s)$$

with \star denoting the redheffer star product. The transfer functions T_{zw} , T_{qw} and T_{zp} correspond to the transfer between the inputs p, w and outputs q, z of the matrix $M(s)$ as in Figure 1, but after closing the loop with the block Δ . If ω_0 is the single active frequency, such that the multiplicity of $\bar{\sigma}(T_{zw}(j\omega_0, \delta))$ is 1, h_∞ is differentiable and, as shown in [2], its derivatives read:

$$\frac{\partial h_\infty}{\partial \delta_i} = -\text{Tr} \left(\text{Re}(T_{qw}(j\omega_0, \delta)) p_{\omega_0} q_{\omega_0}^H T_{zp}(j\omega_0, \delta) \right)^T \Delta_i \quad (19)$$

Where p_{ω_0} and q_{ω_0} are the normalized right and left singular vectors of $T_{zw}(j\omega_0, \delta)$ associated with $\bar{\sigma}(T_{zw}(j\omega_0, \delta))$ (which is equal to $-h_\infty(\delta)$).

From the results of Section II and Proposition 5.b), we deduce that we can use smooth optimization, and in particular SQP (Algorithm 1), to solve Problem (13). In particular, let us define the direction d_δ such that its components are defined as in equation (19) (even when h_∞ is not differentiable), i.e. the i -th component of d_δ reads:

$$d_{\delta,i} = -\text{Tr}(\text{Re}(T_{qw}(j\omega_0, \delta)p_{\omega_0}q_{\omega_0}^H T_{zp}(j\omega_0, \delta))^T \Delta_i)$$

where ω_0 is an active frequency – but not necessarily the only one, and the multiplicity of $\bar{\sigma}(T_{zw}(j\omega_0, \delta))$ is not necessarily 1 – and p_{ω_0} and q_{ω_0} are the corresponding normalized right and left singular vectors of $T_{zw}(j\omega_0, \delta)$. Then, d_δ is a subgradient of h_∞ (this is straightforward from the expression of the subgradient given in [2, Section IV-1]); by Proposition 2 and Theorem 3, it can legitimately be used in SQP as if it were the gradient of a differentiable function.

Remark 3. Proposition 2.b) is not anecdotal in this application. Indeed, after optimization of the controller, it is frequent to have multiple active frequencies. Therefore, it is important for the optimality criterion to be valid at a nonsmooth point, even if the function will most often be differentiable during the optimization.

Remark 4. In contrast, minimizing the lower- C^1 function $-h_\infty(\delta)$, i.e. minimizing the \mathcal{H}_∞ norm, would be a more complex, genuinely nonsmooth problem. In particular, an unconstrained minimum may occur at a point where many subgradients are not zero (as a more simple example, consider $f : x \rightarrow |x|$, which is also lower- C^1). For this problem, nonsmooth techniques in the literature include multidirectional search [32], gradient sampling [33], or Clarke subdifferential-based [3], [34]. This is also pointed out in [2] as a fundamental difference between min-max and min-min (or max-max) programs, the former (e.g. minimizing the \mathcal{H}_∞ norm) being genuinely non-smooth while the latter (e.g. maximizing the \mathcal{H}_∞ norm or equivalently minimizing h_∞) having the favorable properties demonstrated above.

3) Spectral abscissa (function a):

The case of the spectral abscissa is slightly less favorable than the \mathcal{H}_∞ norm. We recall that simple eigenvalues (i.e. those of multiplicity one) are differentiable [35]. As in [2], we call "active eigenvalues" all eigenvalues whose real part is equal to the spectral abscissa.

Proposition 6 (Regularity of a [2], [36])

- a) If all active eigenvalues of $A(\delta)$ are semi-simple (i.e. their algebraic and geometric multiplicity are equal), then a is locally Lipschitz and thus Clarke subdifferentiable at δ .
- b) If all active eigenvalues of $A(\delta)$ are simple at δ , then a is upper- C^1 at δ .
- c) If $A(\delta)$ has only one active eigenvalue and it is simple, then a is differentiable at δ . With the notation of equations (16) and (17), the derivative of a with regard to δ_i reads:

$$\frac{\partial a}{\partial \delta_i} = -\text{Tr}(\Delta_i^T \text{Re}((I - D_{11}\Delta)^{-1} C_1 v_i u_i^H B_1 (I - \Delta D_{11})^{-1})^T) \quad (20)$$

where v_i and u_i are right and left eigenvectors associated with the active eigenvalue, normalized such that $u_i^H v_i = 1$.

Proposition 6.a) was established in [2] following the earlier work of [36]. These references build on the study of [37] concerning the directional derivatives of the spectral abscissa. b) is also shown in [2], it simply follows from the fact that the spectral abscissa is the maximum of the real parts of the eigenvalues, which are differentiable when the eigenvalues are simple [35]. For c), the expression (20) is straightforward from the expression of the Clarke subdifferential given in [2].

Remark 5. Additionally, if there are two active eigenvalues and they are complex conjugate eigenvalues, a is also differentiable and the gradient given above remains valid for either of the two eigenvalues [36].

Remark 6. Although the assumption of semi-simplicity is required for the definition of the Clarke subdifferential, the numerical experiments reported in [2] show that their bundle approach, based on Clarke subdifferentials, performs well in practice even without explicitly verifying this assumption.

Remark 7. As for the \mathcal{H}_∞ norm, minimizing the spectral abscissa is a more complex problem; in the literature, this is addressed with bundle methods [38], [39], gradient bundle [40], gradient sampling [33], Clarke subdifferential-based [36].

In this paper, as for h_∞ , we rely on the upper- C^1 property of a of Proposition 6.b) and on the results of Section II, when active eigenvalues are simple. Our numerical experiments are satisfactory; however, the case of non-simple active eigenvalues is admittedly a limitation of using smooth optimization algorithms for the worst-case search in stability.

C. Choice of optimization algorithms

Problems (12), (13) and (14) are constrained optimization problems involving the nonsmooth functions a , h_∞ , and the differentiable function h_2 . We propose to use either Particle Swarm Optimization or Monte-Carlo sampling for global

exploration of the parametric space, and then Sequential Quadratic Programming for local exploitation. As demonstrated in Section II, this procedure will converge to KKT points of the optimization problems.

1) Sequential Quadratic Programming (SQP):

SQP is described in Algorithm 1 and, as discussed in Section II, may be used to minimize upper- C^1 functions. In our numerical application, we used MATLAB routine FMINCON [41]. In FMINCON, the matrix H of the quadratic problem (10) serves as an approximation of the Hessian matrix of the Lagrangian, iteratively updated with the Broyden-Fletcher-Goldfarb-Shanno (BFGS) method. It is worth noting that BFGS was observed to perform well in [36] even for a non-smooth objective function (the spectral abscissa).

2) Particle swarm optimization (PSO):

PSO is a heuristic global optimization method that handles nonsmooth functions. It only relies on the evaluation of the function and does not depend on (sub)gradient information or on the regularity properties discussed in Section III-B; thus, it may help circumvent limitations encountered when the spectral abscissa fails to be upper- C^1 , or even Clarke subdifferentiable. The nonlinear constraint is treated with a barrier method to penalize non admissible solutions: we reformulate problem (13) as:

$$\begin{aligned} & \underset{\delta \in \mathbb{R}^k}{\text{minimize}} && h_\infty(\delta) + \tau \sum_i \max(0, c_i(\delta)) \\ & \text{subject to} && -1 \leq \delta_i \leq 1 \end{aligned}$$

and problems (12) and (14) can be treated similarly. The parameter τ can be set to a high value, and iteratively increased if necessary until a solution δ^* verifying all constraints $c_i(\delta^*) \leq 0$ is found. The bounds on the δ_i are enforced by projecting the particles positions into the admissible space at each iteration. In our numerical testings, we used MATLAB routine PSO described in [42]; PSO was used as a method to explore the parametric space (and the choice of parameters was done accordingly, as discussed in Section V-C), with local exploitation being performed by a subsequent SQP.

3) Monte-Carlo (MC) sampling:

Monte Carlo sampling is applied as follows: randomly pick a sample δ in the unit hypercube (considering for example uniform distributions for all parameters); evaluate $c(\delta)$: if positive, discard δ , otherwise, evaluate the function $a(\delta)$ (respectively $h_\infty(\delta)$ or $h_2(\delta)$); repeat until having N function evaluations. The worst-case δ^* corresponds to the lowest value of a (respectively h_∞ or $h_2(\delta)$). In our testings, Monte Carlo will also be followed by SQP for local exploitation.

In such a worst-case search problem, the number N of function evaluations can be chosen to verify:

$$N \geq \frac{\ln(\gamma)}{\ln(1 - \epsilon)}$$

where γ and ϵ serve as confidence and accuracy levels to guarantee the probability [10]:

$$\mathbb{P}(\mathbb{P}(f(\delta) > f(\delta^*) \leq \epsilon) \geq 1 - \gamma) \quad (21)$$

for an objective function f (in our case: $a(\delta)$, $h_\infty(\delta)$ or $h_2(\delta)$). Note that this bound is independent from the number of uncertain parameters, from their variation ranges or distributions.

IV. ROBUST CONTROL IN CONSTRAINED PARAMETRIC SPACE

This Section addresses robust controller optimization i.e. problems (1) and (2) in parametric space \mathcal{D} given in (5).

A. Robust controller optimization algorithm

The Algorithm 2, described in a form that solves the standard \mathcal{H}_∞ control problem (1) – the multi-objectives formulation is tackled in Section IV-B – follows the approach proposed in [2] that relies on iteratively constructing a subset $\mathcal{D}_a \subset \mathcal{D}$ of so-called active configurations as follows. Step 1 optimizes the controller for all current active configurations. It uses the nonsmooth optimization algorithm of [3] implemented in the routine SYSTUNE. Step 2 addresses the worst-case search in stability as described in Section III; if a worst-case configuration, i.e. a Karush-Kuhn-Tucker (KKT) point of the optimization problem, is found that leads to a spectral abscissa greater than a tolerance α_{max} , it is added to \mathcal{D}_a . It is also possible to identify multiple KKT points during Step 2. Similarly, Step 3 tackles the worst-case search in performance and adds to \mathcal{D}_a the worst-case configuration(s) that degrade the performance by more than a tolerance ϵ . Finally, Step 4 performs a more exhaustive worst-case search, meaning that the optimization parameters are tuned to increase coverage of the parameter space and ensure a more thorough exploration of potential worst-case configurations, while in Steps 2 and 3 they are chosen to prioritize fast convergence to KKT points; additional quantitative details are provided in the application of Section V-D. For

Steps 2, 3 and 4, the global exploration may be performed either with Particle Swarm Optimization (PSO), or Monte-Carlo (MC) if stochastic guarantees are sought; in both cases, a subsequent Sequential Quadratic Programming (SQP) refines the search until finding a KKT point.

Algorithm 2 Robust control optimization with constrained uncertainties

Initialization: Initialize the set of active configurations as $\mathcal{D}_a = \{0\}$.

Step 1: Multi-model synthesis.

Compute optimal controller $K^* = \arg \min_{K \in \mathcal{K}} \max_{\delta \in \mathcal{D}_a} \|T_{zw}(s, K, \delta)\|_\infty$ using nonsmooth optimization (SYSTUNE).

Step 2: Destabilization.

Identify one or multiple KKT point(s) for the problem: $\delta^* = \arg \max_{\delta \in \mathcal{D}} \alpha(A(K^*, \delta))$ using PSO/MC+SQP.

If $\alpha(A(K^*, \delta)) > \alpha_{max}$, add δ^* to \mathcal{D}_a and go back to step 1.

Otherwise continue to step 3.

Step 3: Degrade performance.

Identify one or multiple KKT point(s) for the problem: $\delta^* = \arg \max_{\delta \in \mathcal{D}} \|T_{zw}(s, K^*, \delta)\|_\infty$ using PSO/MC+SQP.

If a destabilizing δ is found during this optimization, go back to step 2 and start SQP directly from δ .

Else, if $\|T_{zw}(s, K^*, \delta^*)\|_\infty > (1 + \epsilon) \max_{\delta \in \mathcal{D}_a} \|T_{zw}(s, K^*, \delta)\|_\infty$, add δ^* to \mathcal{D}_a and go back to step 1.

Otherwise, go to step 4.

Step 4: Validation

Perform exhaustive worst-case search in stability and performance.

If a configuration δ^* not respecting criteria of step 2 or 3 is found, add δ^* to \mathcal{D}_a and go back to step 1.

Otherwise, terminate.

B. Multi-objective formulation

Algorithm 2 is presented to address the standard problem formulation (1) involving a single \mathcal{H}_∞ criterion. We note that this formulation also directly addresses the multi-objective problem:

$$\underset{K \in \mathcal{K}}{\text{minimize}} \quad \max_{1 \leq i \leq n} \max_{\delta \in \mathcal{D}} \alpha_i \|T_{z_i w_i}(s, K, \delta)\|_\infty$$

since it is equivalent to a single objective problem (e.g. as in [43], [1]):

$$\max_{1 \leq i \leq n} \max_{\delta \in \mathcal{D}} \alpha_i \|T_{z_i w_i}(s, K, \delta)\|_\infty = \max_{\delta \in \mathcal{D}} \|\text{diag}(\alpha_i T_{z_i w_i}(s, K, \delta))\|_\infty. \quad (22)$$

In our numerical implementation, we used the expression on the left side of equation (22); indeed, it was faster to compute the norm of each requirement, than the norm of the block diagonal system.

More generally, we consider the multi-objectives problem (2). As explained in [44], the controller optimization of Step 1 treats it as :

$$\underset{K \in \mathcal{K}}{\text{minimize}} \quad \max \left\{ \max_{\delta \in \mathcal{D}} \|T_{z_1 w_1}(s, K, \delta)\|, \eta \max_{2 \leq i \leq n} \max_{\delta \in \mathcal{D}} \|T_{z_i w_i}(s, K, \delta)\| \right\}$$

where $\|\cdot\|$ may refer to the \mathcal{H}_2 or \mathcal{H}_∞ system norm, and where η is adjusted during the optimization with a penalty approach. In our worst-case performance searches (in Steps 3 and 4), we use the following normalization, such that the performance degradation test of Step 3 (i.e. $\|T_{zw}(s, K^*, \delta^*)\|_\infty > (1 + \epsilon) \max_{\delta \in \mathcal{D}_a} \|T_{zw}(s, K^*, \delta)\|_\infty$, in the single objective case) becomes, in the multi-objectives case:

$$\max \left\{ \frac{1}{(1 + \epsilon_1)\beta} \max_{\delta \in \mathcal{D}} \|T_{z_1 w_1}(s, K, \delta)\|, \frac{1}{(1 + \epsilon_2)} \max_{2 \leq i \leq n} \max_{\delta \in \mathcal{D}} \|T_{z_i w_i}(s, K, \delta)\| \right\} > 1 \quad (23)$$

where β is the soft performance obtained in Step 1:

$$\beta = \max_{\delta \in \mathcal{D}_a} \|T_{z_1 w_1}(s, K^*, \delta)\|$$

i.e. the algorithm has converged when the worst-case search degrades the soft requirement by less than $1 + \epsilon_1$, and the hard requirements are less than $1 + \epsilon_2$. Finally, we point out that, in our implementation, the PSO computes all norms involved in equation (23) and determines their maximum; whereas the subsequent SQP only evaluates the transfer function that achieved this maximum.

V. APPLICATION: A LARGE FLEXIBLE SPACECRAFT

A. Plant model and uncertain parameters

The benchmark used in this study is designed to be challenging regarding robustness. We consider a spacecraft composed of one rigid body connected to two large flexible solar panels. The clamped-free natural frequencies are 0.20, 0.50, 0.75 and 0.85 rad/s for each panel. The resulting 8 nominal free-free frequencies are between 0.20 and 4.2 rad/s for the whole spacecraft. Uncertainties are considered on various mechanical properties:

- Each clamped-free frequency exhibits a common 10% across both panels, along with an additional 5% asymmetric uncertainty. Modal damping is 0.001 for each clamped-free mode.
- The mass, center of mass, inertia (MCI) properties of the solar panel are uncertain, as well as the modal participation factors of the flexible modes.
- The angle between the central body and the solar arrays may have any value between $-\pi$ and $+\pi$.
- The central body also has uncertain MCI properties.
- We also consider an uncertain stiffness and damping in the rotation of the solar array, as a simple solar array driving mechanism (SADM) model.

In total, there are 43 uncertain parameters δ_i (normalized such that $-1 \leq \delta_i \leq 1$, without loss of generality) regrouped in a vector δ . Noting $M_P(\delta)$ the mass matrix at attachment point P of a solar panel, and $L_P(\delta)$ the matrix of modal participation factors, the robustness analysis should exclude any configuration δ such that the residual mass matrix defined in equation (24) is not positive definite (indeed, such configurations do not represent a physical system). Hence the nonlinear constraint:

$$M_r(\delta) := M_P(\delta) - L_P^T(\delta)L_P(\delta) \succeq 0 \quad (24)$$

which can also be written under a scalar form:

$$c(\delta) := \alpha(-M_r(\delta)) \leq 0. \quad (25)$$

The spacecraft model $G(s, \delta)$ is built with the multibody approach detailed in [45] and implemented in the Satellite Dynamics Toolbox Library (SDTlib) [46], [47]. The block Δ_G of the Linear Fractional Representation (LFR) model, such that $G(s, \delta) = \mathcal{F}_u(M_G(s), \Delta_G)$ (upper LFT), has size 204. We emphasize that this model contains all parametric configurations in a continuous manner, defined at each subsystem level based on the physics equations without any interpolation or other approximation (besides the linearity assumption). The LFR model of the spacecraft includes all configurations for $-1 \leq \delta_i \leq 1$ even though only $\sim 22\%$ of them respect the nonlinear constraint (25).

Remark 8. In addition to providing the analytical expressions of the gradients given in Section III, the LFR representation also enables fast model evaluation at given parametric configuration by simply substituting the Δ_G block.

B. Closed loop and control problem

The benchmark focuses on the attitude control of the satellite described above to follow a reference r . The control input u of the plant $G(s, \delta)$ is the torque applied to the satellite (e.g. by reaction wheels, thrusters...) and the output vector contains the 3 angle measurements polluted by some noise n . The closed loop is represented in Figure 2, where $d(s)$ represents avionics: a 2-nd order Pade approximation of a 0.125s delay, and a 2-nd order low-pass filter with a cut-off frequency of 10 rad/s representing actuator dynamics. We note $\mathcal{K}(s)$ the set of controllers $K(s)$ of the desired structure: one 4-th order controller per spacecraft axis, each one taking the measured angle and rate as inputs and generating a control torque, resulting in 24 decision parameters per controller (72 in total). The closed-loop plant has 50 states.

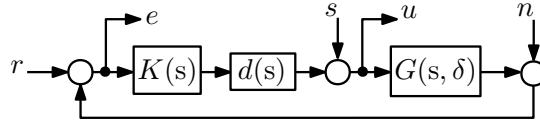


Fig. 2: Benchmark: closed-loop system

The control problem consists in placing a control bandwidth of 0.1 rad/s (hence interacting with the uncertain flexible modes) while ensuring a modulus margin of 0.5 and minimizing the variance of the actuator command in response to measurement noise. It reads:

$$\begin{aligned} & \underset{K \in \mathcal{K}}{\text{minimize}} && \max_{\delta \in \mathcal{D}} \|T_{n \rightarrow u}(s, K, \delta)\|_2^2 \\ & \text{subject to} && \max_{\delta \in \mathcal{D}} \|\frac{1}{2}T_{s \rightarrow u}(s, K, \delta)\|_\infty < 1 \\ & && \max_{\delta \in \mathcal{D}} \|WT_{r \rightarrow e}(s, K, \delta)\|_\infty < 1 \\ & && \max_{\delta \in \mathcal{D}} \alpha(A(K, \delta)) < -10^{-7} \end{aligned} \quad (26)$$

where \mathcal{D} is defined in (5) with the nonlinear constraint (25), the factor $\frac{1}{2}$ in the 2nd requirement ensures the desired modulus margin, and $W = \frac{10s+1}{2(10s+0.01)}I_3$ is a weighting filter to impose the desired bandwidth of 0.1 rad/s. The last requirement of problem (26) ensures closed-loop stability with some tolerance, where $A(K, \delta)$ is the matrix A of the state-space representation of the closed-loop system.

C. Worst-case search

In this section, we present the worst-case search for the spectral abscissa and the \mathcal{H}_∞ norm, as presented in Section III. We selected three controllers K_1, K_2, K_3 obtained at early iterations of the robust controller tuning presented in Section V-D and analyze the robustness of the closed-loop system with three Test cases. The tests are ran on a 12th Gen Intel(R) Core(TM) i7-12700H 2.30 GHz, with 14 cores and 16GB of RAM. Computation times are provided for reference, but they may vary depending on hardware, software configuration, implementation details, optimization parameters, etc.

1) Test case 1: spectral abscissa (multiple local optima):

Test case 1 illustrates how the proposed approaches perform in presence of several local optima, in different regions of the parametric space, that are not particularly rare. We search for $\max_{\delta \in \mathcal{D}} \alpha(A(K_1, \delta))$.

a) SQP

We ran the Sequential Quadratic Programming (SQP) algorithm from 100 random initial points. As termination criteria, we set 10^{-6} as optimality tolerance (KKT stationarity condition), and 10^{-8} as step tolerance (step size between two iterations). The resulting worst-case spectral abscissas $\alpha(A(\delta_{\text{SQP}}^*)) = -a(\delta_{\text{SQP}}^*)$ of each run are in Figure 3a, and suggest the presence of several local optima, which highlights the limitation of such a local method. These various local optima may correspond to significantly different parametric configurations. For example, the worst case 0.135 has the value -1.0 for the (normalized) value of one of the moments of inertia of the solar panel, -0.09 and 1.0 for the modal participation factors of the clamped-free modes 1 and 3 in rotation around the same axis; in contrast, the local optimum 0.007 has -0.30, -1.0 and -0.87 respectively for these three parameters. Figure 3b presents the poles map for the initial poles (for the random initialization of the parameters) and final poles (corresponding to the worst case) for one of the runs that converged to the suggested global optimum.

Excluding the runs that did not detect instability (each of which took less than 0.1s), the remaining runs took between 2.5 and 78s (average: 21s – regarding total computation time, we recall that each SQP run is inherently sequential, but that the 100 runs are executed in parallel).

b) PSO, PSO + SQP

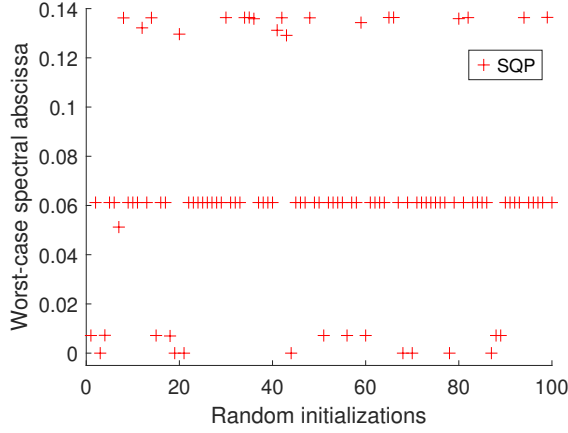
The parameters of the Particle Swarm Optimization (PSO) were chosen as follows to favor global exploration over local exploitation. We set a range of 0.6 to 1.1 for the adaptive inertias ('InertiaRange' option in MATLAB). Iterations terminate when performance is increased by less than 10% ('FunctionTolerance') across 20 last iterations ('MaxStallIterations'). For a given computational budget, because PSO is sensitive to initialization [48], running several independent instances with different initializations can yield better results than increasing the number of particles or tightening the termination tolerance. Therefore, we performed 100 independent runs with the parameters given above, each with 500 particles ('SwarmSize') – cf. also [49] for a discussion on population size in PSO. All other parameters were set to MATLAB's default settings. Bearing in mind that our parameter choices were specifically tuned for multiple fast independent runs rather than to maximize the reliability of a single run, the results should be interpreted to determine how many such runs are required to reliably identify a worst case. We see that, with a few runs, we are able to consistently identify the worst-case configuration that was most often missed by the local SQP alone.

For each run, the computations of the 500 particles were parallelized over 14 cores. Each run took between 6s and 8s (average: 7s) with 11000 model evaluations. Each run was followed by SQP (starting from the identified worst case), each between 37 and 97s (average: 77s); these SQPs were parallelized. The results in Figure 3c show that the (suggested) global optimum can be consistently found using a few random initializations of PSO+SQP.

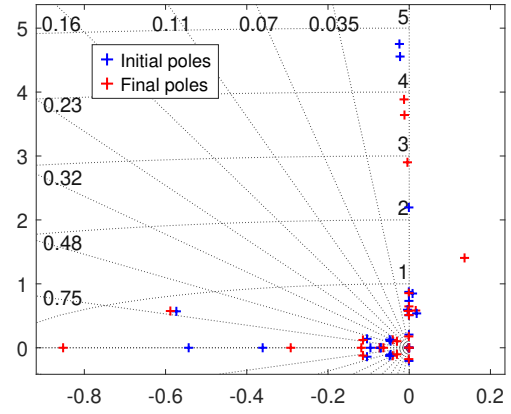
c) MC, MC + SQP

To enable a fair comparison with PSO, (i) we performed a total of $N_{\text{MC}} = 1.1\text{e}6$ evaluations of the objective function a , matching the total number of objective function evaluations of the PSO across all 100 runs, and (ii) we divided the N_{MC} random samples into 100 groups, that we call Monte-Carlo (MC) experiments. MC performed almost as well as PSO, cf. Figure 3d. In all runs, the subsequent SQP significantly improves the result. Each MC run took about 6.2s, and the SQP runtimes were similar to the PSO case.

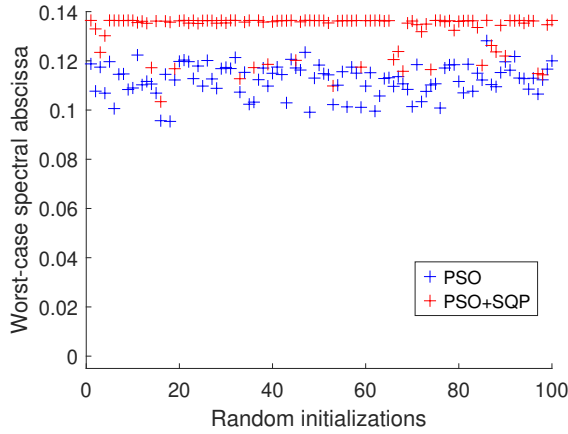
We mention that 78% of the drawn samples were not admissible ($c(\delta) > 0$) and were therefore discarded before evaluation of $a(\delta)$. About 92% of the admissible configurations were destabilizing ($a(\delta) < 0$). We also mention that the total number



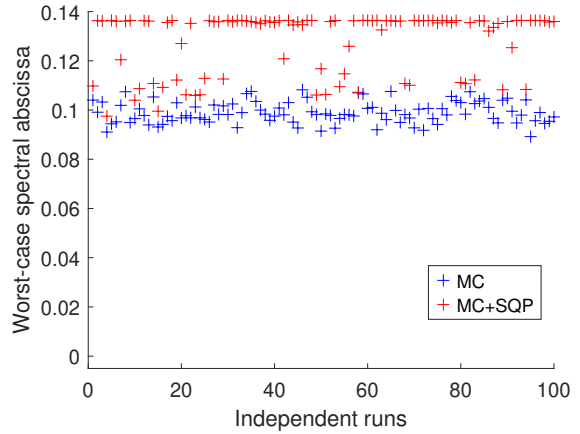
(a) SQP, with 100 random initializations



(b) Poles map (zoomed) for a SQP run



(c) PSO and PSO+SQP, with random 100 initializations



(d) MC and MC+SQP, repeated 100 times

Fig. 3: Worst-case spectral abscissa for Test case 1

of runs N_{MC} verifies $N_{MC} \approx \ln(\gamma)/\ln(1 - \epsilon)$ with the values $\gamma = \epsilon = 1e-5$, which guarantees as in equation (21) that the worst-case $a(\delta_{MC}^*)$ found through all samples of Figure 3d (without considering the subsequent SQP) covers 99.999% of the probability distribution of $a(\delta)$ with a confidence level of 99.999%. These observations suggest that the worst case around 0.136 is rare, even though unstable configurations are frequent in Test case 1.

2) Test case 2: spectral abscissa (rare worst case):

Test case 2 illustrates how the proposed approaches perform when the destabilization is rare. Indeed, only $\sim 0.018\%$ of the admissible parametric space (as approximated by the MC experiments) yields instability of $A(K_2, \delta)$. We search for $\max_{\delta \in \mathcal{D}} \alpha(A(K_2, \delta))$.

Most SQP runs remained stuck on the local optimum $\alpha(A(\delta_{SQP}^*)) = -a(\delta_{SQP}^*) = -2e^{-7}$ that occupies most of the parametric space (Figure 4a). On the other hand, PSO+SQP (Figure 4c) more consistently finds the destabilizing configurations. PSO runs required more function evaluations than Test case 1: 1525500 across the 100 runs, for a runtime ranging from 6s to 57s with an average of 11s. MC (again executed with the same total number of objective function evaluations as PSO for fair comparison) is also able to detect instability (Figure 4d), but it is significantly outperformed by PSO (compare the blue crosses of Figures 4c and 4d). MC+SQP performs decently but is slightly less reliable than PSO+SQP.

3) Test case 3: \mathcal{H}_∞ norm:

For controller K_3 , we applied the methods of Test cases 1 and 2 and did not find any destabilizing configuration for $A(K_3, \delta)$. Thus, we search for the worst-case \mathcal{H}_∞ norm: $\max_{\delta \in \mathcal{D}} \|\frac{1}{2}T_{s \rightarrow u}(s, K_3, \delta)\|_\infty$ (2nd control requirement of Problem (26)). We note that the objective function is longer to evaluate than in previous Test cases 1 and 2.

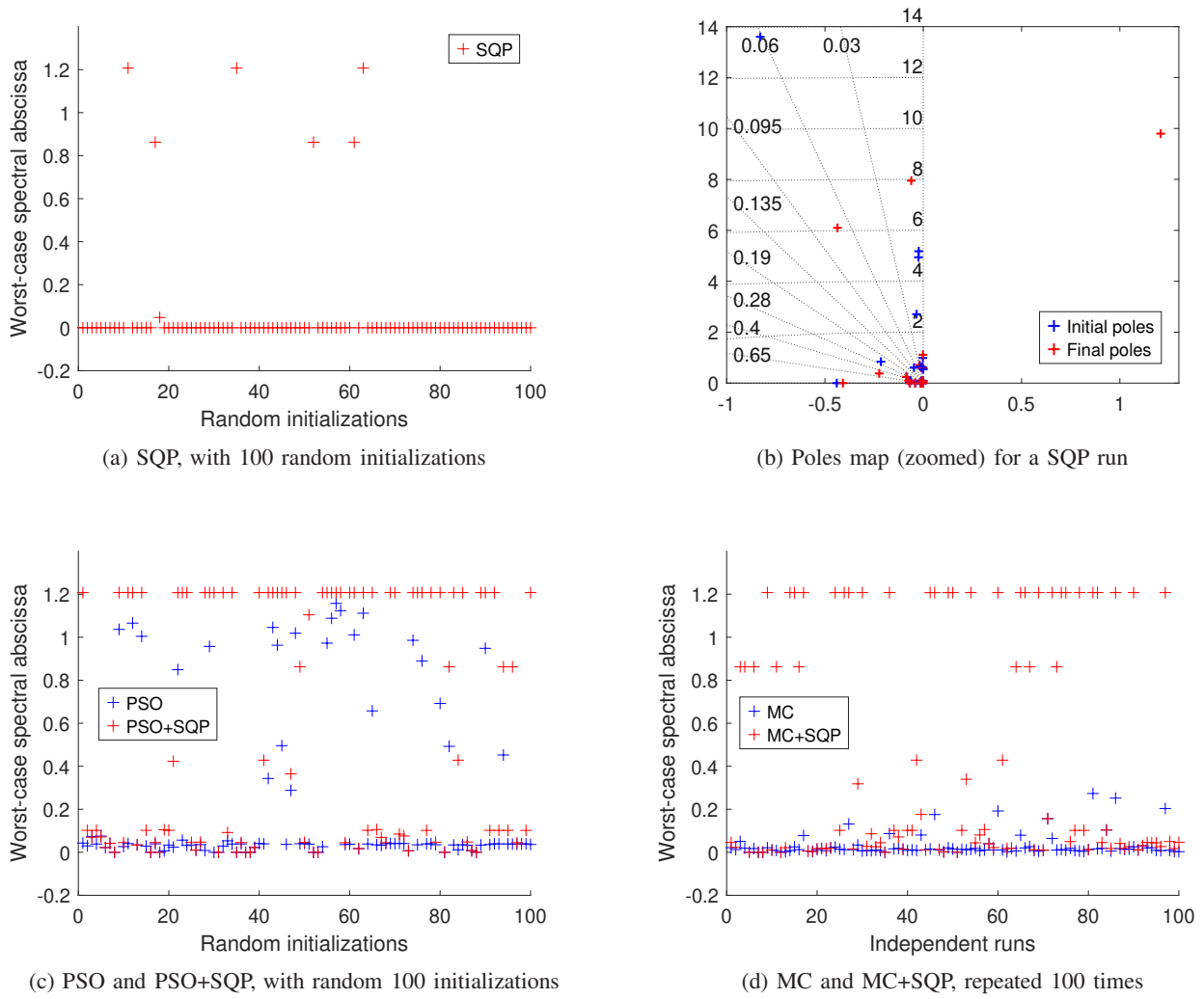


Fig. 4: Worst-case spectral abscissa for Test case 2

The results are shown in Figure 5. The SQP runs took between 38s and 1172s (average: 591s). The PSO individual runtimes ranged from 72 to 126s (average: 85s), and MC around 95s on average. Here, PSO tends to get stuck in the local optimum 1.15, whereas MC+SQP more frequently converges to the suggested global optimum. In both cases, the subsequent SQP improves the result of PSO or MC alone.

D. Robust control

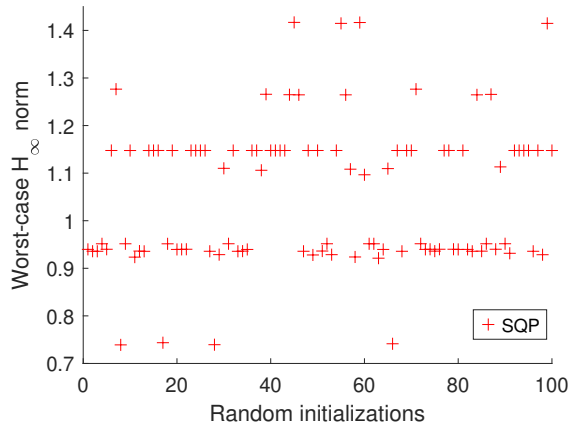
In this section, we solve Problem (26) using Algorithm 2.

1) Implementation details:

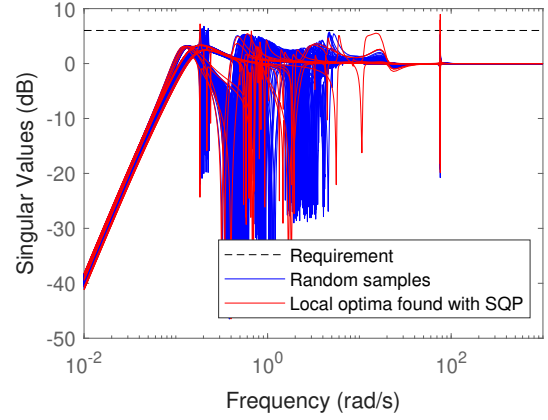
In the following, let us call *problematic configuration* any configuration that does not respect the criterion of either Step 2 (i.e. such that $\alpha(A(K^*, \delta)) > \alpha_{min}$) or Step 3 (i.e. such that $\|T_{zw}(s, K^*, \delta^*)\|_\infty > (1 + \epsilon) \max_{\delta \in \mathcal{D}_a} \|T_{zw}(s, K^*, \delta)\|_\infty$ or its multi-objectives counterpart of equation (23)). Below we give implementation details regarding the various steps of Algorithm 2.

Step 1: Multi-models controller synthesis

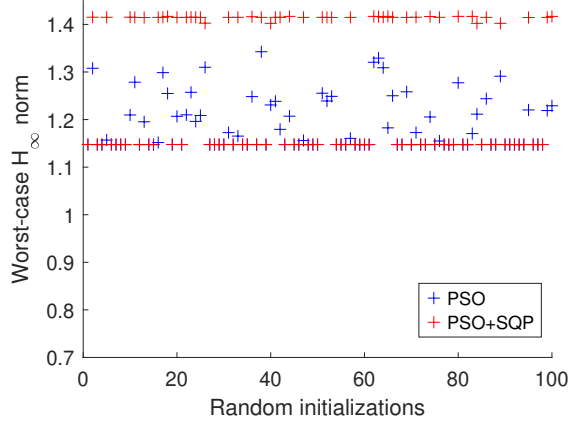
SYSTUNE is initialized with the controller obtained at previous iteration along with 13 random initializations. If no satisfactory controller is found, the process is repeated with new random initializations until one is obtained. In principle, a maximum number of attempts could be enforced to declare the problem infeasible, but this option was not activated, as a feasible solution was always found in our experiments.



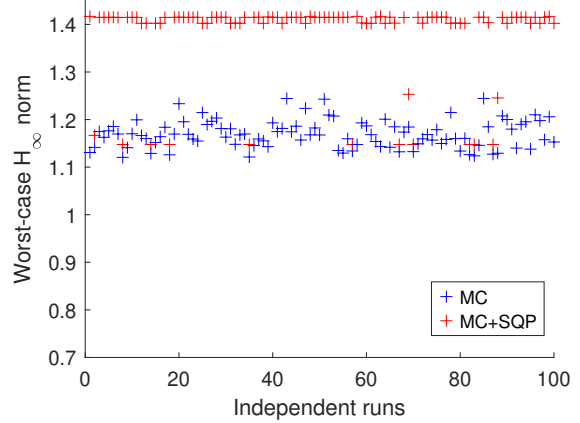
(a) SQP, with 100 random initializations



(b) Sigma plot: 100 random samples and a few KKT points



(c) PSO and PSO+SQP, with random 100 initializations



(d) MC and MC+SQP, repeated 100 times

Fig. 5: Worst-case (normalized) \mathcal{H}_∞ norm for Test case 3

Steps 2 and 3: Worst-case searches

Compared to the choice of parameters of Section V-C, here we reduced the swarm size to 100 and we relaxed the PSO convergence criterion: iterations terminate when performance is increased by less than 10% across 10 last iterations. For SQP, we reduced the step tolerance from $1e-8$ to $1e-6$. The objective is to speed up the detection of active configurations in most iterations, relying on Step 4 to perform a finer validation. Below, we present three different strategies for the worst-case searches.

Strategy 1

We run a single instance of PSO, followed by SQP. Although, as seen in Section V-C, this does not always converge to the global optimum, we prioritize computational speed by stopping at the first KKT point for several reasons. First, each KKT point may be valuable to add to the active configurations even if it is not the global worst-case for the current controller. Second, because multiple iterations are performed, any missed problematic configuration can be detected in subsequent iterations. Third, if stability is validated in Step 2 but a destabilizing configuration is discovered when degrading performance in Step 3, the process returns to Step 2. Fourth, a more exhaustive search is carried out in Step 4, allowing a return to previous iterations if a problematic configuration is identified, while limiting the number of such more expensive searches. The resulting (single) KKT point, if problematic, is added to the active configurations.

Strategy 2

Strategy 2 is the same as Strategy 1, except that the PSO is stopped as soon as a problematic configuration is found (using 'ObjectiveLimit' option in MATLAB); the PSO is then followed by SQP.

Strategy 3

In Strategy 3, we perform 4 instances of PSO+SQP and obtain 4 KKT points δ_i^* . For clarity, let us assume that they are

all problematic configurations. The worst case among those 4, noted δ_1^* , is added to the active configurations. Then, we compute the distance $|\delta_2^* - \delta_1^*|$; if the distance exceeds a specified threshold, δ_2^* is also added to the active configurations. The procedure is repeated for δ_3^* and δ_4^* : each δ_i^* is added to the active scenarios only if its distance from all previously selected points exceeds the threshold. The threshold is chosen as half of the hypercube diagonal of the parameter space, i.e., \sqrt{k} , where k is the number of uncertain parameters. This choice limits the number of active scenarios by enforcing a minimum spatial separation, thereby ensuring that only significantly distinct worst-case configurations are retained. Indeed, the computation time of the multi-models controller synthesis (Step 1) increases with the number of active configurations.

Step 4: validation

In Step 4, we run up to N instances of PSO. If a problematic configuration is found, we run SQP, and add the resulting worst case to the active configurations. Otherwise, we run SQP on all N instances. In other words, Step 4 operates like Section V-C when no problematic configuration is found, but terminates earlier when one is identified. This procedure is applied for both the stability and performance, and the Algorithm 2 terminates when no problematic configuration is found. In the implementation, we conducted the worst-case search for performance before that for stability to avoid unnecessary computations, since performance was observed to fail more frequently than stability. We used the same optimization parameters as in Section V-C and $N = 20$, which is deemed sufficient to ensure thorough validation of the robustness.

2) Results:

As in section V-C, the tests are ran on a 12th Gen Intel(R) Core(TM) i7-12700H 2.30 GHz, with 14 cores and 16GB of RAM, and computation times are provided for reference. We used the tolerances $\epsilon_1 = 5\%$ and $\epsilon_2 = 1\%$ (cf. equation (23)).

The Algorithm 2 was executed 5 times for each strategy. All runs converged to a robust controller. Table I presents a few averaged metrics for comparison. The runtime of the final validation (Step 4) is averaged over all 15 runs, because this step is conducted identically for each strategy. As the multi-models controller synthesis (Step 1) becomes increasingly long when the number of active configurations increases, Strategy 2 results in the longest runtime. Indeed, although it saves time by prematurely stopping the PSO, the resulting KKT point is typically not a global optimum, which in turn requires a larger number of active configurations to ensure robustness. Strategy 3, which may add multiple KKT points to the active configurations at each iteration, results in less iterations and a reduced total runtime.

Figure 6 presents the transfer functions of Problem (26) after optimization of the controller. Active configurations (in red) include the worst cases detected in the final iteration.

TABLE I: Controller optimization results

Metrics	Strategy 1	Strategy 2	Strategy 3
Nb of iterations (= nb. of executions of Step 1) (min/avg/max)	7/8.4/10	11/12.2/17	6/7.4/10
Nb. of active configurations (min/avg/max)			7/8.6/12
Total runtime, excluding final validation (avg)	4034s	4919s	3708s
... including % represented by controller tuning (Step 1)	34%	58%	33%
... including % represented by worst-case searches (Steps 2 and 3)	66%	42%	67%
Runtime of the final validation (Step 4 – stability) (avg)	139s		
Runtime of the final validation (Step 4 – performance) (avg)	2332s		

VI. CONCLUSION

This paper focused on the robust control and worst-case search in presence of nonlinear constraints restricting the hypercube. This specificity is missing from the current state of the art, and arises for example when considering uncertain mechanical properties e.g. in flexible satellites.

Relying on the theory of upper- C^1 functions, we established favorable properties that justify the use of smooth optimization algorithms for these nonsmooth problems: any subgradient defines a valid descent direction, local optima satisfy the Karush–Kuhn–Tucker (KKT) conditions for all subgradients, and sequential quadratic programming converges to KKT points when applied to such functions. This theoretical foundation legitimizes the use of standard, readily available optimization tools, which is of practical importance for industrial users.

To perform the worst-case search, we combined Particle Swarm Optimization (or Monte-Carlo sampling, if stochastic guarantees are desired) for global exploration and Sequential Quadratic Programming for local exploitation. Numerical experiments on a flexible spacecraft benchmark show that this method significantly outperforms Monte-Carlo sampling alone, and is able to reliably detect even rare worst-case configurations. Then, by iteratively constructing a set of active configurations, multi-objectives robust controller optimization was performed in reasonable runtime.

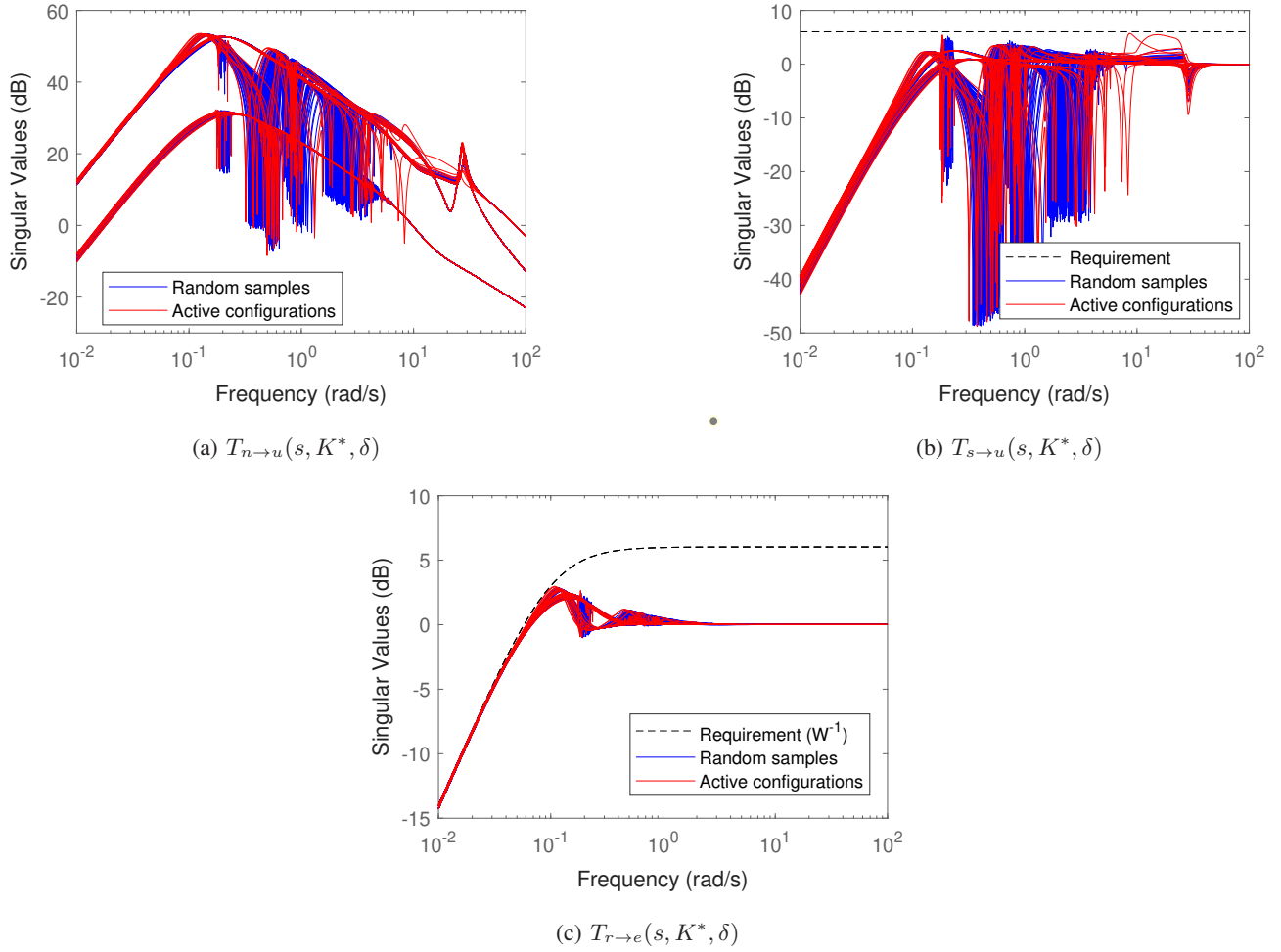


Fig. 6: Transfer functions in Problem (26) after controller optimization, with active configurations and 100 random samples

Finally, we emphasize that the proposed worst-case search, performing global exploration and being compatible with a large number of uncertain parameters and states, has the potential to complement existing robust control techniques, including in the unconstrained case.

FUNDING SOURCES

This work was funded par Région Occitanie in the frame of the France 2030 program. Ce projet a été financé par la Région Occitanie dans le cadre de France 2030.

ACKNOWLEDGMENTS

The authors acknowledge the use of an AI tool (ChatGPT: GPT-4) to assist in the reformulation of certain sentences.

REFERENCES

- [1] P. Apkarian and D. Noll, “The H infinity Control Problem is Solved,” *Aerospace Lab*, no. 13, pp. 1–27, 2017.
- [2] P. Apkarian, M. N. Dao, and D. Noll, “Parametric Robust Structured Control Design,” *IEEE Transactions on Automatic Control*, vol. 60, no. 7, pp. 1857–1869, 2015, arXiv: 1405.4202 Publisher: IEEE.
- [3] P. Apkarian and D. Noll, “Nonsmooth H infinity synthesis,” *IEEE Transactions on Automatic Control*, vol. 51, no. 1, pp. 71–86, 2006.
- [4] F. Clarke, *Optimization and nonsmooth analysis*, ser. Society for industrial and Applied Mathematics, 1990.
- [5] S. Boyd and C. Barratt, *Linear Controller Design: Limits of Performance*, ser. Englewood Cliffs, NJ: Prentice Hall., 1991.
- [6] J. Doyle, “Analysis of feedback systems with structured uncertainties,” *IEE Proceedings D Control Theory and Applications*, vol. 129, no. 6, p. 242, 1982. [Online]. Available: <https://digital-library.theiet.org/content/journals/10.1049/ip-d.1982.0053>
- [7] C. Roos, “Systems modeling, analysis and control (SMAC) toolbox: An insight into the robustness analysis library,” in *2013 IEEE Conference on Computer Aided Control System Design (CACSD)*. Hyderabad, India: IEEE, Aug. 2013, pp. 176–181. [Online]. Available: <http://ieeexplore.ieee.org/document/6663479/>
- [8] J.-M. Biannic, C. Roos, S. Bennani, F. Boquet, V. Preda, and B. Girouart, “Advanced probabilistic mu -analysis techniques for AOCS validation,” *European Journal of Control*, vol. 62, pp. 120–129, Nov. 2021. [Online]. Available: <https://linkinghub.elsevier.com/retrieve/pii/S0947358021000789>

- [9] F. Somers, C. Roos, J. Biannic, F. Sanfedino, V. Preda, S. Bennani, and H. Evain, "Delay Margin Analysis of Uncertain Linear Control Systems Using Probabilistic mu," *International Journal of Robust and Nonlinear Control*, vol. 35, no. 6, pp. 2101–2118, Apr. 2025. [Online]. Available: <https://onlinelibrary.wiley.com/doi/10.1002/rnc.7780>
- [10] R. Tempo, E. Bai, and F. Dabbene, "Probabilistic robustness analysis: explicit bounds for the minimum number of samples," in *Proceedings of 35th IEEE Conference on Decision and Control*, vol. 3. Kobe, Japan: IEEE, 1996, pp. 3424–3428. [Online]. Available: <http://ieeexplore.ieee.org/document/573690/>
- [11] J. E. Spingarn, "Submonotone subdifferentials of Lipschitz functions," vol. 264, no. 1, 1981.
- [12] J. Nocedal and S. J. Wright, *Numerical optimization*, second edition ed., ser. Springer series in operations research and financial engineering. New York, NY: Springer, 2006.
- [13] J. Kennedy and R. Eberhart, "Particle swarm optimization," in *Proceedings of ICNN'95 - International Conference on Neural Networks*, vol. 4. Perth, WA, Australia: IEEE, 1995, pp. 1942–1948. [Online]. Available: <http://ieeexplore.ieee.org/document/488968/>
- [14] M. Davenport and M. Egerstedt, "Convex optimization - Course notes," [Online]. Available: <https://mdav.ece.gatech.edu/ece-6270-spring2021/notes/>
- [15] E. Kassarian, F. Sanfedino, D. Alazard, J. Montel, and C.-A. Chevrier, "Modeling of stratospheric balloons and robust line-of-sight pointing control," *CEAS Space Journal*, Jul. 2023. [Online]. Available: <https://link.springer.com/10.1007/s12567-023-00515-x>
- [16] E. Kassarian, F. Sanfedino, D. Alazard, and H. Evain, "Parametric sensitivity analysis for the robust control of uncertain space systems," in *EuroGNC*, Bristol, 2024.
- [17] M. Martin, S. Winkler, F. Belien, and R. Forstner, "Towards new V&V in AOCS/GNC for industrial efficiency," in *ESA-GNC 2023*, 2023.
- [18] M. Martin, S. Winkler, F. Belien, and R. Förstner, "Sample-based sensitivity analysis for uncertain AOCS verification and validation," *CEAS Space Journal*, Jul. 2025. [Online]. Available: <https://link.springer.com/10.1007/s12567-025-00619-6>
- [19] F. Sanfedino, P. Iannelli, D. Alazard, and E. Pelletier, "European Satellite Benchmark for Control Education & Industrial Training - Lesson Learned in the Control Design of a Fine Pointing Mission," 2025. [Online]. Available: <https://ssrn.com/abstract=5231029>
- [20] L. Szerdahelyi, S. Fugger, P. Espeillac, G. Monroig, T. Pareaud, and M. Casasco, "The BepiColombo attitude and orbit control system," in *Proceedings of the 9th ESA-GNC conference*, Porto, Portugal, 2014.
- [21] A. Falcoz, C. Pittet, S. Bennani, A. Guignard, C. Bayart, and B. Frapard, "Systematic design methods of robust and structured controllers for satellites: Application to the refinement of Rosetta's orbit controller," *CEAS Space Journal*, vol. 7, no. 3, pp. 319–334, Sep. 2015. [Online]. Available: <http://link.springer.com/10.1007/s12567-015-0099-8>
- [22] C. Charbonnel, "H?? Controller Design and m-Analysis: Powerful Tools for Flexible Satellite Attitude Control," in *AIAA Guidance, Navigation, and Control Conference*. Toronto, Ontario, Canada: American Institute of Aeronautics and Astronautics, Aug. 2010. [Online]. Available: <https://arc.aiaa.org/doi/10.2514/6.2010-7907>
- [23] M. N. Dao, "Bundle Method for Nonconvex Nonsmooth Constrained Optimization," *Journal of convex analysis*, vol. 22, no. 4, pp. 1061–1090, 2015.
- [24] P. Apkarian and D. Noll, "Worst-case stability and performance with mixed parametric and dynamic uncertainties," *International Journal of Robust and Nonlinear Control*, vol. 27, no. 8, pp. 1284–1301, May 2017. [Online]. Available: <https://onlinelibrary.wiley.com/doi/10.1002/rnc.3628>
- [25] W. De Oliveira, "Short Paper - A note on the Frank-Wolfe algorithm for a class of nonconvex and nonsmooth optimization problems," *Open Journal of Mathematical Optimization*, vol. 4, pp. 1–10, Jan. 2023. [Online]. Available: <https://ojmo.centre-mersenne.org/articles/10.5802/ojmo.21/>
- [26] S. P. Han, "A globally convergent method for nonlinear programming," *Journal of Optimization Theory and Applications*, vol. 22, pp. 297–309, 1977.
- [27] M. J. D. Powell, "Variable Metric Methods for Constrained Optimization," in *Mathematical Programming The State of the Art*, A. Bachem, B. Korte, and M. Grötschel, Eds. Berlin, Heidelberg: Springer Berlin Heidelberg, 1983, pp. 288–311. [Online]. Available: http://link.springer.com/10.1007/978-3-642-68874-4_12
- [28] K. Zhou, J. C. Doyle, and K. Glover, *Robust and Optimal Control*. Englewood Cliffs: Prentice hall, 1996, iSSN: 09670661.
- [29] T. Rautert and E. W. Sachs, "Computational Design of Optimal Output Feedback Controllers," *SIAM Journal on Optimization*, vol. 7, no. 3, pp. 837–852, Aug. 1997. [Online]. Available: <http://epubs.siam.org/doi/10.1137/S1052623495290441>
- [30] P. Apkarian, D. Noll, and A. Rondepierre, "Mixed H2/Hinfinity control via nonsmooth optimization," in *Proceedings of the 48th IEEE Conference on Decision and Control (CDC) held jointly with 2009 28th Chinese Control Conference*. Shanghai, China: IEEE, Dec. 2009, pp. 6460–6465. [Online]. Available: <http://ieeexplore.ieee.org/document/5400165/>
- [31] D. Arzelier, D. Georgia, S. Gumussoy, and D. Henrion, "H2 for HIFOO," Oct. 2010, arXiv:1010.1442 [math]. [Online]. Available: <http://arxiv.org/abs/1010.1442>
- [32] P. Apkarian and D. Noll, "Controller Design via Nonsmooth Multidirectional Search," *SIAM Journal on Control and Optimization*, vol. 44, no. 6, pp. 1923–1949, Jan. 2006. [Online]. Available: <http://epubs.siam.org/doi/10.1137/S0363012904441684>
- [33] J. V. Burke, A. S. Lewis, and M. L. Overton, "A Robust Gradient Sampling Algorithm for Nonsmooth, Nonconvex Optimization," *SIAM Journal on Optimization*, vol. 15, no. 3, pp. 751–779, Jan. 2005. [Online]. Available: <http://epubs.siam.org/doi/10.1137/030601296>
- [34] V. Bompard, D. Noll, and P. Apkarian, "Second-order nonsmooth optimization for H infinity synthesis," *Numerische Mathematik*, vol. 107, no. 3, pp. 433–454, Aug. 2007. [Online]. Available: <http://link.springer.com/10.1007/s00211-007-0095-9>
- [35] M. L. Overton and R. S. Womersley, "On Minimizing the Special Radius of a Nonsymmetric Matrix Function: Optimality Conditions and Duality Theory," *SIAM Journal on Matrix Analysis and Applications*, vol. 9, no. 4, pp. 473–498, Oct. 1988. [Online]. Available: <http://epubs.siam.org/doi/10.1137/0609040>
- [36] V. Bompard, P. Apkarian, and D. Noll, "Non-smooth techniques for stabilizing linear systems," in *2007 American Control Conference*. New York, NY, USA: IEEE, Jul. 2007, pp. 1245–1250. [Online]. Available: <http://ieeexplore.ieee.org/document/4282408/>
- [37] J. V. Burke and M. L. Overton, "Differential properties of the spectral abscissa and the spectral radius for analytic matrix-valued mappings," *Nonlinear Analysis: Theory, Methods & Applications*, vol. 23, no. 4, pp. 467–488, Aug. 1994. [Online]. Available: <https://linkinghub.elsevier.com/retrieve/pii/0362546X94900906>
- [38] F. Oustry, "A second-order bundle method to minimize the maximum eigenvalue function," *Mathematical Programming*, vol. 89, no. 1, pp. 1–33, Nov. 2000. [Online]. Available: <http://link.springer.com/10.1007/PL00011388>
- [39] D. Noll and P. Apkarian, "Spectral bundle methods for non-convex maximum eigenvalue functions. Part 1: first-order methods," vol. 104, pp. 701–727, 2005.
- [40] J. V. Burke, A. S. Lewis, and M. L. Overton, "Two numerical methods for optimizing matrix stability," *Linear Algebra and its Applications*, vol. 351–352, pp. 117–145, Aug. 2002. [Online]. Available: <https://linkinghub.elsevier.com/retrieve/pii/S0024379502002604>
- [41] "Constrained Nonlinear Optimization Algorithms, MATLAB help page," 2025. [Online]. Available: <https://fr.mathworks.com/help/optim/ug/constrained-nonlinear-optimization-algorithms.html>
- [42] "Particle swarm optimization algorithm, MATLAB help page," 2025. [Online]. Available: <https://fr.mathworks.com/help/gads/particle-swarm-optimization-algorithm.html>
- [43] P. Apkarian and D. Noll, "Nonsmooth optimization for multidisk H infinity synthesis," *European Journal of Control*, vol. 12, no. 3, pp. 229–244, 2006.
- [44] P. Apkarian, P. Gahinet, and C. Buhr, "Multi-model, multi-objective tuning of fixed-structure controllers," in *2014 European Control Conference (ECC)*. Strasbourg, France: IEEE, Jun. 2014, pp. 856–861. [Online]. Available: <http://ieeexplore.ieee.org/document/6862200/>

- [45] D. Alazard, C. Cumer, and K. Tantawi, "Linear dynamic modeling of spacecraft with various flexible appendages and on-board angular momentums," *7th International ESA Conference on Guidance, Navigation and Control Systems*, vol. 41, no. 2, pp. 11 148–11 153, 2008, iISBN: 9783902661005.
- [46] D. Alazard and F. Sanfedino, "Satellite Dynamics Toolbox for Preliminary Design Phase," *43rd Annual AAS Guidance and Control Conference*, vol. 172, pp. 1461–147, 2020.
- [47] F. Sanfedino, D. Alazard, E. Kassarian, and F. Somers, "Satellite Dynamics Toolbox Library: a tool to model multi-body space systems for robust control synthesis and analysis," in *IFAC PapersOnline*, Mar. 2023.
- [48] Q. Li, S.-Y. Liu, and X.-S. Yang, "Influence of initialization on the performance of metaheuristic optimizers," *Applied Soft Computing*, vol. 91, p. 106193, Jun. 2020. [Online]. Available: <https://linkinghub.elsevier.com/retrieve/pii/S1568494620301332>
- [49] A. P. Piotrowski, J. J. Napiorkowski, and A. E. Piotrowska, "Population size in Particle Swarm Optimization," *Swarm and Evolutionary Computation*, vol. 58, p. 100718, Nov. 2020. [Online]. Available: <https://linkinghub.elsevier.com/retrieve/pii/S2210650220303710>
- [50] P. Apkarian, D. Noll, and L. Ravanbod, "Nonsmooth Bundle Trust-region Algorithm with Applications to Robust Stability," *Set-Valued and Variational Analysis*, vol. 24, no. 1, pp. 115–148, Mar. 2016. [Online]. Available: <http://link.springer.com/10.1007/s11228-015-0352-5>
- [51] J. W. Daniel, "Stability of the solution of definite quadratic programs," *Mathematical Programming*, vol. 5, no. 1, pp. 41–53, Dec. 1973. [Online]. Available: <http://link.springer.com/10.1007/BF01580110>
- [52] F. Clarke, Y. Ledyae, R. Stern, and P. Wolenski, *Nonsmooth analysis and control theory*. Springer New York.

APPENDIX

In this Appendix, we prove the propositions of Section II. For readability, they are reminded before introducing the proofs.

Proposition 1 (Descent directions and optimality of upper- C^1 functions – Unconstrained case)

Let a locally Lipschitz function f be upper- C^1 at x , and $g_x \in \partial f(x)$ any subgradient of f at x . We consider Problem (6).
a) *Descent direction.* Any direction $-g_x$, with $g_x \in \partial f(x)$ such that $\|g_x\| \neq 0$, is a descent direction for $f(x)$, and in particular it verifies $f'(x, -g_x) \leq -\|g_x\|^2 < 0$ where $f'(x, d)$ denotes the the directional derivative at x in direction d .
b) *Optimality.* If x (locally) minimizes $f(x)$, then $\|g_x\| = 0$ for any $g_x \in \partial f(x)$.

Proof. The proof is provided in the body of the paper. □

Proposition 2 (Descent directions and optimality of upper- C^1 functions – Constrained case)

Let a locally Lipschitz function f be upper- C^1 at x , and $g_x \in \partial f(x)$ any subgradient of f at x . Let the c_i be continuously differentiable. We consider Problem (8).

a) *Descent direction.* Let (p, u) be a KKT pair of $Q(x, H, g_x)$. If $\|p\| \neq 0$ and $\|u\|_\infty \leq r$, then p is a descent direction for $\theta_r(x)$, i.e. $\theta'_r(x, p) < 0$ where $\theta'_r(x, d)$ denotes the the directional derivative at x in direction d .
b) *Optimality.* If x (locally) minimizes $f(x)$ subject to n constraints $c_i(x) \leq 0$ (Problem (8)), then any $g_x \in \partial f(x)$ verifies the following KKT conditions: there exists $(\mu_i)_{1 \leq i \leq n}$ such that:

$$\begin{aligned} g_x + \sum_{i=1}^n \mu_i \nabla c_i(x) &= 0 \\ \forall i, \mu_i \geq 0, \mu_i c_i(x) &= 0, c_i(x) \leq 0 \end{aligned}$$

Proof. a) The proof of a) is an adaptation of [26, Theorem 3.1], originally written for a differentiable f , to the upper- C^1 case. Let us define:

$$I = \{i : c_i(x) > 0\}, \bar{I} = \{i : c_i(x) = 0\}, \hat{I} = \{i : c_i(x) < 0\}$$

As in [26] we have:

$$\theta'_r(x, p) = f'(x, p) + r \sum_{i \in I} \nabla c_i(x)^T p + r \sum_{i \in \bar{I}} (\nabla c_i(x)^T p)_+.$$

Since f is upper- C^1 , we have $f'(x, p) = \min_{g \in \partial f(x)} \langle g, p \rangle \leq g_x^T p$ and thus

$$\theta'_r(x, p) \leq g_x^T p + r \sum_{i \in I} \nabla c_i(x)^T p + r \sum_{i \in \bar{I}} (\nabla c_i(x)^T p)_+.$$

In the original proof of [26, Theorem 3.1], the expression above is an equality with $\nabla f(x)$ instead of g_x . From there, the proof of [26, Theorem 3.1] is identical, as follows. Since (p, u) is a KKT pair of $Q(x, H, g_x)$, we have $c_i(x) + \nabla c_i(x)^T p \leq 0$ which yields:

$$\sum_{i \in \bar{I}} (\nabla c_i(x)^T p)_+ = 0$$

and since $u_i(c_i(x) + \nabla c_i(x)^T p) = 0$, we deduce:

$$\theta'_r(x, p) \leq g_x^T p + \sum_{i=1}^n u_i \nabla c_i(x)^T p + \sum_{i=1}^n u_i c_i(x) + r \sum_{i \in I} \nabla c_i(x)^T p.$$

Since (p, u) is a KKT pair of $Q(x, H, g_x)$ we also have:

$$g_x + \sum_{i=1}^n u_i \nabla c_i(x) + \frac{1}{2}(H + H^T)p = 0$$

and noticing that $\sum_{i \in \bar{I} \cup \hat{I}}^n u_i c_i(x) \leq 0$ yields:

$$\begin{aligned} \theta'_r(x, p) &\leq -\frac{1}{2}(H + H^T)p + \sum_{i \in I}^n (c_i(x) + r \nabla c_i(x)^T p) \\ &\leq -\frac{1}{2}(H + H^T)p + \sum_{i \in I}^n (u_i - r) c_i(x) \\ &< 0 \end{aligned}$$

since H is positive definite and $|u|_\infty < r$.

b) is proved in the body of the paper. □

To prove Proposition 3, we first introduce the following lemmas.

Lemma 1 (Supermonotonicity of the subdifferential of upper- C^1 functions)

Let f be upper- C^1 at x . For every $\epsilon > 0$, there exists $\delta > 0$ such that for all $x_0, x'_0 \in \mathcal{B}(x, \delta)$:

$$(g_{x'_0} - g_{x_0})^T (x'_0 - x_0) \leq \epsilon \|x'_0 - x_0\|$$

where $g_{x_0} \in \partial f(x_0)$ and $g_{x'_0} \in \partial f(x'_0)$.

Proof. This comes from [11, Theorem 3.9] (submonotonicity of the subdifferential of lower- C^1 functions) and is also noted for example in [50, Lemma 6]. □

Lemma 2 (Perturbation of a quadratic problem) Let us consider the two quadratic problems:

$$\begin{aligned} x_0 &= \arg \min \left\{ Q(x) = \frac{1}{2}x^T Kx - x^T k, \text{ subject to } Gx \leq g \right\} \\ x'_0 &= \arg \min \left\{ Q'(x) = \frac{1}{2}x^T K'x - x^T k', \text{ subject to } G'x \leq g' \right\} \end{aligned}$$

where K, K' are symmetric, positive definite matrices. Let us partition G in matrices A, B and g in vectors a, b such that $Bx \leq b$ is always satisfied as an equality while $Ax \leq a$ can be satisfied with strict inequality. Let us define similarly B' in the partition of G' and suppose that $\text{rank}(B) = \text{rank}(B')$. Set $\epsilon = \max \left(\|K - K'\|, \|G - G'\|, \|g - g'\|, \frac{(k' - k)^T (x'_0 - x_0)}{\|x'_0 - x_0\|} \right)$. Then there exists $\epsilon_0 > 0$ and $c > 0$ such that:

$$\|x'_0 - x_0\| \leq c\epsilon$$

whenever $\epsilon < \epsilon_0$.

Proof. This lemma is an adaptation of [51] where, instead of our assumption $(k' - k)^T (x'_0 - x_0) \leq \epsilon \|x'_0 - x_0\|$, the stronger assumption $\|k' - k\| \leq \epsilon$ was considered. Let us note $\lambda > 0$ the smallest eigenvalue of K . Let us first demonstrate the equivalent of [51, Theorem 2.1], i.e., that in the unconstrained case:

$$x_0 = \arg \min \left\{ Q(x) = \frac{1}{2}x^T Kx - x^T k \right\}, \quad x'_0 = \arg \min \left\{ Q'(x) = \frac{1}{2}x^T K'x - x^T k' \right\}$$

we have:

$$\|x'_0 - x_0\| \leq \epsilon(\lambda - \epsilon)^{-1}(1 + \|x_0\|).$$

The proof for this statement is almost identical to the one provided in [51, Theorem 2.1], as follows. For any $x \in \mathbb{R}^k$, we have:

$$(x - x_0)^T \nabla Q(x_0) \geq 0$$

$$(x - x'_0)^T \nabla Q'(x'_0) \geq 0$$

with the gradients $\nabla Q(x) = Kx - k$ and $\nabla Q(x) = K'x - k'$. Substituting $x = x'_0$ and $x = x_0$ respectively in these two equations and adding the results yields

$$(x'_0 - x_0)^T (\nabla Q(x_0) - \nabla Q'(x'_0)) \geq 0$$

which is equivalent to

$$(x'_0 - x_0)^T (\nabla Q'(x'_0) - \nabla Q'(x_0)) \leq (x'_0 - x_0)^T (\nabla Q(x_0) - \nabla Q'(x_0))$$

For the left side:

$$\begin{aligned} (x'_0 - x_0)^T (\nabla Q'(x'_0) - \nabla Q'(x_0)) &= (x'_0 - x_0)^T K'(x'_0 - x_0) \\ &\geq (\lambda - \epsilon) \|x'_0 - x_0\|^2 \end{aligned}$$

For the right side:

$$\begin{aligned} (x'_0 - x_0)^T (\nabla Q(x_0) - \nabla Q'(x_0)) &= (x'_0 - x_0)^T (K - K')x_0 + (x'_0 - x_0)^T (k' - k) \\ &\leq \epsilon \|x'_0 - x_0\| (\|x_0\| + 1) \end{aligned}$$

which finalizes the proof for the unconstrained case. Note that the only difference with the original proof of [51, Theorem 2.1] is that they used $(x'_0 - x_0)^T (k' - k) \leq \|x'_0 - x_0\| \cdot \|k' - k\|$ to deduce $(x'_0 - x_0)^T (k' - k) \leq \epsilon \|x'_0 - x_0\|$, whereas it was directly our assumption.

Then, the rest of the proof provided in [51] still holds. Indeed, the propositions [51, Propositions 3.1, 3.2] only tackle the constrained sets, and do not involve k or k' . Moreover, in, [51, Section 4], the relationship between k and k' is not used (except when using [51, Theorem 2.1], which we generalized already); in fact, [51, Section 4] only works on $Q(x)$. \square

Proposition 3 (Convergence of SQP for upper- C^1 functions)

Let f be upper- C^1 and the c_i be continuously differentiable. Assume that the following conditions are satisfied:

(i) there exists $\alpha, \beta > 0$ such that, for each k and for any $x \in \mathbb{R}^k$:

$$\alpha x^T x \leq x^T H_k x \leq \beta x^T x$$

(ii) For each k , there exists a KKT point of $Q(x_k, H_k, g_{x_k})$ (equation (10)) with a Lagrange multiplier vector u_k such that $\|u_k\|_\infty \leq r$.

Then, any sequence (x_k) generated by Algorithm 1 either terminates at a KKT point of the constrained optimization problem (8), or any accumulation point \bar{x} with

$$S^0(\bar{x}) = \{p : c(\bar{x}) + \nabla c(\bar{x})^T p < 0\} \neq \emptyset$$

is a KKT point of Problem (8).

Proof. Once again, we follow the proof of [26, Theorem 3.2] and adapt it to the case where f is not differentiable but only upper- C^1 . For completeness, we reproduce the entire proof and indicate where our modified assumptions apply, while emphasizing that the proof itself is not our own.

By assumption (ii), (p_k, u_k) is a KKT pair of $Q(x_k, H_k, g_{x_k})$ with $\|u_k\|_\infty \leq r$. If $p_k = 0$, then (x_k, u_k) satisfies the KKT conditions (9) of Problem (8) and the algorithm can terminate at x_k .

Thus, for the following, we assume that $p_k \neq 0$. From Proposition 2.a) (originally [26, Theorem 3.1], which we adapted to upper- C^1 functions), it is possible to choose x_{k+1} as described in Algorithm 1, and in particular, it verifies:

$$\theta_r(x_{k+1}) < \theta_r(x_k) + \epsilon_k.$$

Let \bar{x} be an accumulation point of (x_k) with $S^0(\bar{x}) \neq \emptyset$. Without loss of generality (passing to the subsequence if necessary) we may assume

$$x_k \rightarrow \bar{x}, H_k \rightarrow \bar{H}$$

where the existence of \bar{H} follows from assumption (i).

In the original proof [26], the continuity of the gradient of f ensures that $\nabla f(x_k)$ converges to $\nabla f(\bar{x})$. Here, a similar property is maintained as follows. Since f is locally Lipschitz, its subgradients (g_{x_k}) are uniformly bounded for k sufficiently large, hence there exists a subsequence that converges to a vector \bar{g} . Without loss of generality (passing to the subsequence if necessary) we note

$$g_{x_k} \rightarrow \bar{g},$$

and the upper semi-continuity of the Clarke subdifferential [52, Proposition 1.5] yields $\bar{g} \in \partial f(\bar{x})$. Since \bar{H} is positive definite and $S^0(\bar{x}) \neq \emptyset$, the quadratic problem $Q(\bar{x}, \bar{H}, \bar{g})$ (originally $Q(\bar{x}, \bar{H}, \nabla f(\bar{x}))$ in [26]) has a unique KKT point \bar{p} .

If $\bar{p} = 0$, then \bar{x} is a KKT point of Problem (8) and the theorem follows. Thus, we now assume that $\bar{p} \neq 0$ and we will show that this leads to a contradiction.

From the continuity of $\nabla g(x)$, and by Lemmas 1 and 2, where x_{k+1} and x_k play the roles of x_0 and x'_0 , and g_{x_0} and $g_{x'_0}$ play the roles of k and k' , we deduce that:

$$p_k \rightarrow \bar{p}$$

In the original proof [26], this follows [51] (the equivalent to our Lemma 2) and the continuity of $\nabla f(x)$ instead (which is stronger than our Lemma 1).

Since (u_k) is uniformly bounded by r , it has an accumulation point \bar{u} . We note

$$u_k \rightarrow \bar{u}$$

with $\|\bar{u}\|_\infty \leq r$. By passing to the limit in the KKT relation, which is valid for any k , we obtain that \bar{u} is a Lagrange multiplier of $Q(\bar{x}, \bar{H}, \bar{g})$.

The rest of the proof of [26] is unchanged, and is as follows. Let $\bar{\lambda} \in [0, \lambda_{max}]$ be chosen such that

$$\theta_r(\bar{x} + \bar{\lambda}\bar{p}) = \min_{0 \leq \lambda \leq \lambda_{max}} \theta_r(\bar{x} + \lambda\bar{p}).$$

Let us set

$$\gamma = \theta_r(\bar{x} + \bar{\lambda}\bar{p}) - \theta_r(\bar{x}) > 0$$

which is strictly positive by Proposition 2.a). Since $x_k + \bar{\lambda}p_k \rightarrow \bar{x} + \bar{\lambda}\bar{p}$, for sufficiently large k we have:

$$\theta_r(x_k + \bar{\lambda}p_k) + \gamma/2 < \theta_r(\bar{x}).$$

However, for all k we have $\theta_r(x_{k+1}) < \theta_r(x_k) + \epsilon_k$, and for sufficiently large k we have

$$\sum_{i=k}^{\infty} \epsilon_i < \gamma/2$$

which leads to:

$$\begin{aligned} \theta_r(\bar{x}) &< \theta_r(x_{k+1}) + \sum_{i=k+1}^{\infty} \epsilon_i \\ &\leq \min_{0 \leq \lambda \leq \lambda_{max}} \theta_r(x_k + \lambda p_k) + \epsilon_k + \sum_{i=k+1}^{\infty} \epsilon_i \\ &< \theta_r(x_k + \bar{\lambda}p_k) + \gamma/2 \end{aligned}$$

which contradicts the previous inequality $\theta_r(x_k + \bar{\lambda}p_k) + \gamma/2 < \theta_r(\bar{x})$. This proves that $\bar{p} = 0$ and that \bar{x} is a KKT point of Problem (8). \square